Natural products of *Picea* endophytes from the Acadian forest

David R. McMullin[†]

Blake D. Green[†]

Natasha C. Prince[†]

Joey B. Tanney[†]

J. David Miller[†*]

[†] *Ottawa Carleton Institute of Chemistry, Carleton University, 1125 Colonel By Drive, Ottawa, Ontario, Canada, K1S 5B6*

**Corresponding author. E-mail: david.miller@carleton.ca*

Supporting Information

Table S1. Collection information for studied endophytes

Figure S1. Bayesian 50% majority rule ITS consensus tree showing relationship of DAOMC 251461 with related Rhytismataceae species. All unlabeled branches have Bayesian posterior probability values of 1.0; values lower than 1.0 are presented at nodes. The tree is rooted to *Chlorencoelia versiformis* and scale bar indicates expected changes per site per branch.

Figure S2. Bayesian 50% majority rule ITS consensus tree showing relationship of DAOMC 250863 with related Mycosphaerellaceae species. All unlabeled branches have Bayesian posterior probability values of 1.0; values lower than 1.0 are presented at nodes. The tree is rooted to *Zasmidium fructicola* and sequences from ex-type specimens are bold. Scale bar indicates expected changes per site per branch.

Figure S3. ^{1}H (400 MHz, CD_3OD) NMR spectrum for rhytismatone A (**1**)
Figure S4. ^{13}C (100 MHz, CD_3OD) NMR spectrum for rhytismatone A (**1**)
Figure S5. ^{1}H (400 MHz, CD_3OD) NMR spectrum for rhytismatone B (**2**)
Figure S6. ^{13}C (100 MHz, CD_3OD) NMR spectrum for rhytismatone B (**2**)
Figure S7. ^{1}H (400 MHz, CD_3OD) NMR spectrum for (**3**)
Figure S8. ^{13}C (100 MHz, CD_3OD) NMR spectrum for (**3**)
Figure S9. ^{1}H (400 MHz, CD_3OD) NMR spectrum for (**4**)
Figure S10. ^{13}C (100 MHz, CD_3OD) NMR spectrum for (**4**)
Figure S11. ^{1}H (400 MHz, CD_3OD) NMR spectrum for (**5**)
Figure S12. ^{13}C (100 MHz, CD_3OD) NMR spectrum for (**5**)
Figure S13. ^{1}H (400 MHz, CD_3OD) NMR spectrum for (**6**)
Figure S14. ^{13}C (100 MHz, CD_3OD) NMR spectrum for (**6**)
Figure S15. ^{1}H (400 MHz, CD_3OD) NMR spectrum for tyrosol (**7**)
Figure S16. ^{13}C (100 MHz, CD_3OD) NMR spectrum for tyrosol (**7**)
Figure S17. ^{1}H (400 MHz, CD_3OD) NMR spectrum for chloromycorrhizinone A (**8**)
Figure S18. ^{13}C (100 MHz, CD_3OD) NMR spectrum for chloromycorrhizinone A (**8**)
Figure S19. ^{1}H (400 MHz, CD_3OD) NMR spectrum for (1'*Z*)-dechloromycorrhizin A (**9**)
Figure S20. ^{13}C (100 MHz, CD_3OD) NMR spectrum for (1'*Z*)-dechloromycorrhizin A (**9**)
Figure S21. ^{1}H (400 MHz, CD_3OD) NMR spectrum for mycorrhizin A (**10**)
Figure S22. ^{13}C (100 MHz, CD_3OD) NMR spectrum for mycorrhizin A (**10**)
Figure S23. ^{1}H (400 MHz, CD_3OD) NMR spectrum for chloromycorrhizin A (**11**)
Figure S24. ^{13}C (100 MHz, CD_3OD) NMR spectrum for chloromycorrhizin A (**11**)
Figure S25. ^{1}H (400 MHz, CD_3OD) NMR spectrum for (**12**)
Figure S26. ^{13}C (100 MHz, CD_3OD) NMR spectrum for (**12**)
Figure S27. ^{1}H (400 MHz, CD_3OD) NMR spectrum for (**13**)
Figure S28. ^{13}C (100 MHz, CD_3OD) NMR spectrum for (**13**)
Figure S29. ^{1}H (400 MHz, CD_3OD) NMR spectrum for (**14**)
Figure S30. ^{13}C (100 MHz, CD_3OD) NMR spectrum for (**14**)
Figure S31. ^{1}H (400 MHz, CD_3OD) NMR spectrum for (**15**)
Figure S32. ^{13}C (100 MHz, CD_3OD) NMR spectrum for (**15**)

**Corresponding author. E-mail: david.miller@carleton.ca*

**Corresponding author. E-mail: david.miller@carleton.ca*

Table S1. Collection information for studied endophytes

Strain	Identification	Host/substrate	Location	Collection Date	GenBank No.	
					ITS	LSU
DAOMC 251461	Rhytismataceae sp.	*Picea mariana* endophyte	Gagetown, New Brunswick, Canada	18-Jun-13	KY200578	KY200582
DAOMC 250863	Mycosphaerellaceae sp.	*Picea mariana* endophyte	Doaktown, New Brunswick, Canada	21-Jun-13	KY200577	KY200581
DAOMC 250862	*Pezicula sporulosa*	*Picea rubens* endophyte	Fundy National Park, New Brunswick, Canada	24-Sep-13	KY200576	KY200580
DAOMC 250335	*Lachnum* cf. *pygmaeum*	*Picea rubens* fallen twig	Gagetown, New Brunswick, Canada	14-Jun-13	KY200575	KY200579

Figure S1. Bayesian 50% majority rule ITS consensus tree showing relationship of DAOMC 251461 with related Rhytismataceae species. All unlabeled branches have Bayesian posterior probability values of 1.0; values lower than 1.0 are presented at nodes. The tree is rooted to *Chlorencoelia versiformis* and scale bar indicates expected changes per site per branch.

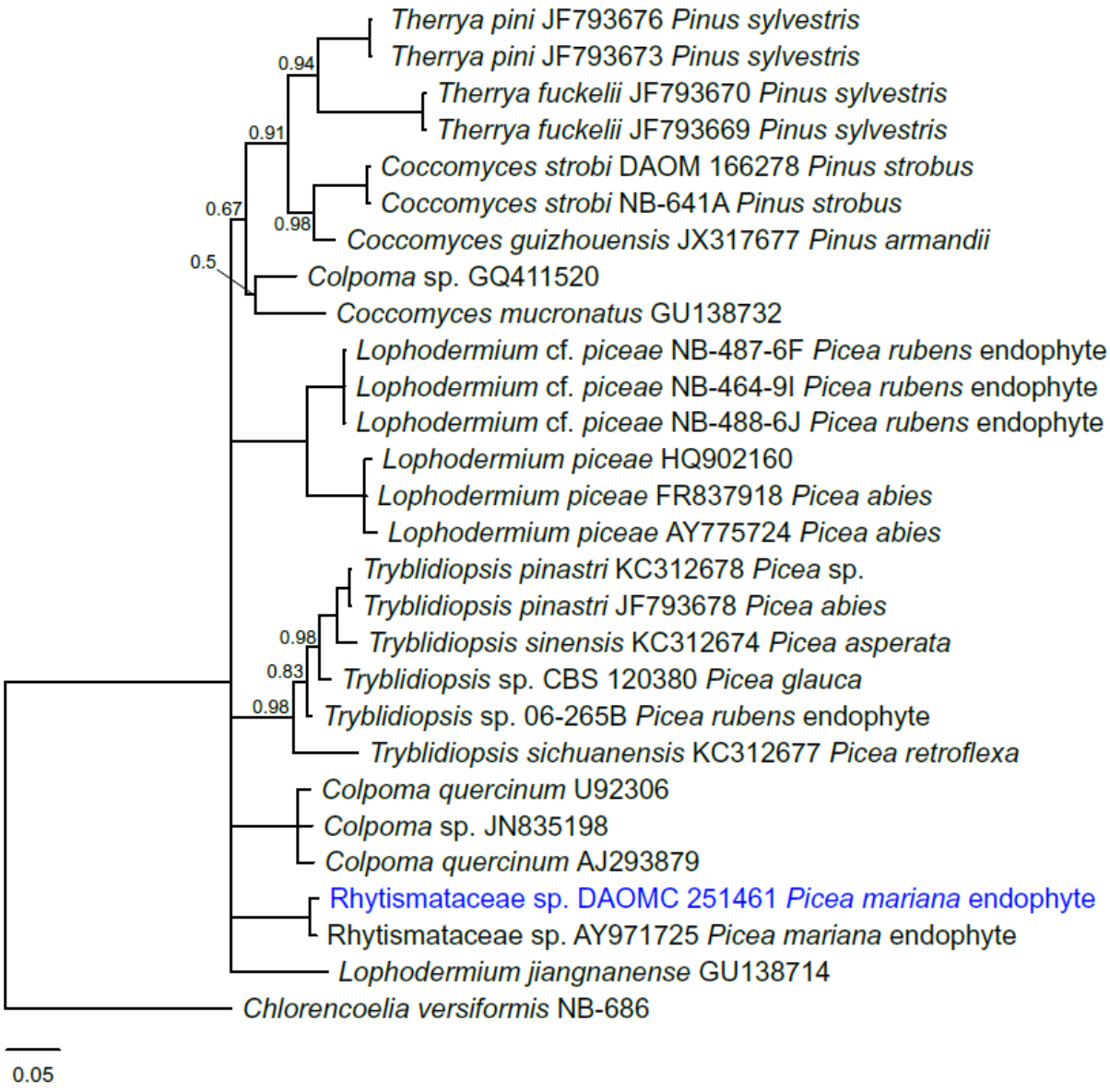

Figure S2. Bayesian 50% majority rule ITS consensus tree showing relationship of DAOMC 250863 with related Mycosphaerellaceae species. All unlabeled branches have Bayesian posterior probability values of 1.0; values lower than 1.0 are presented at nodes. The tree is rooted to *Zasmidium fructicola* and sequences from ex-type specimens are bold. Scale bar indicates expected changes per site per branch.

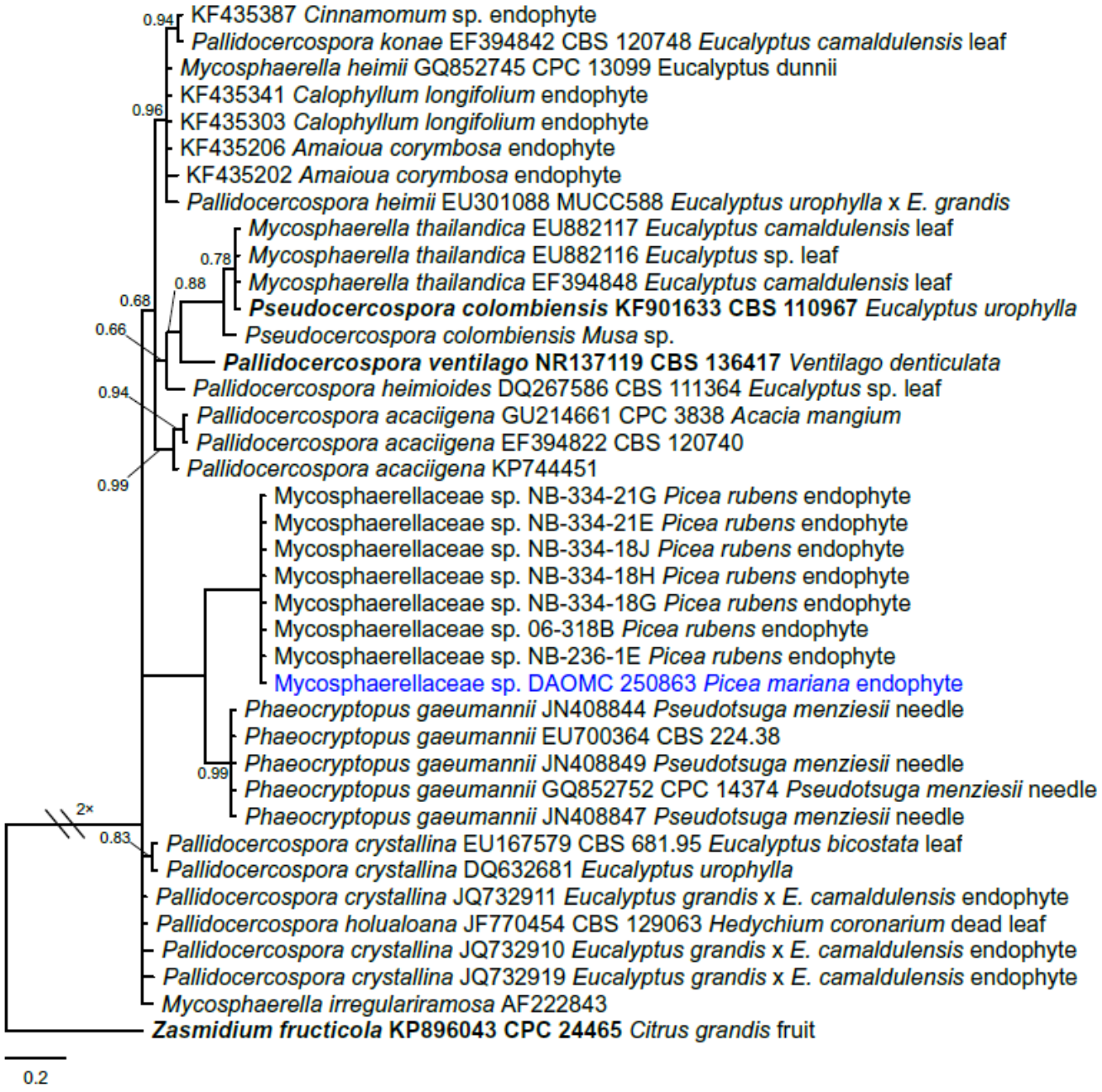

Figure S3. ^{1}H (400 MHz, CD_3OD) NMR spectrum for rhytismatone A (**1**)

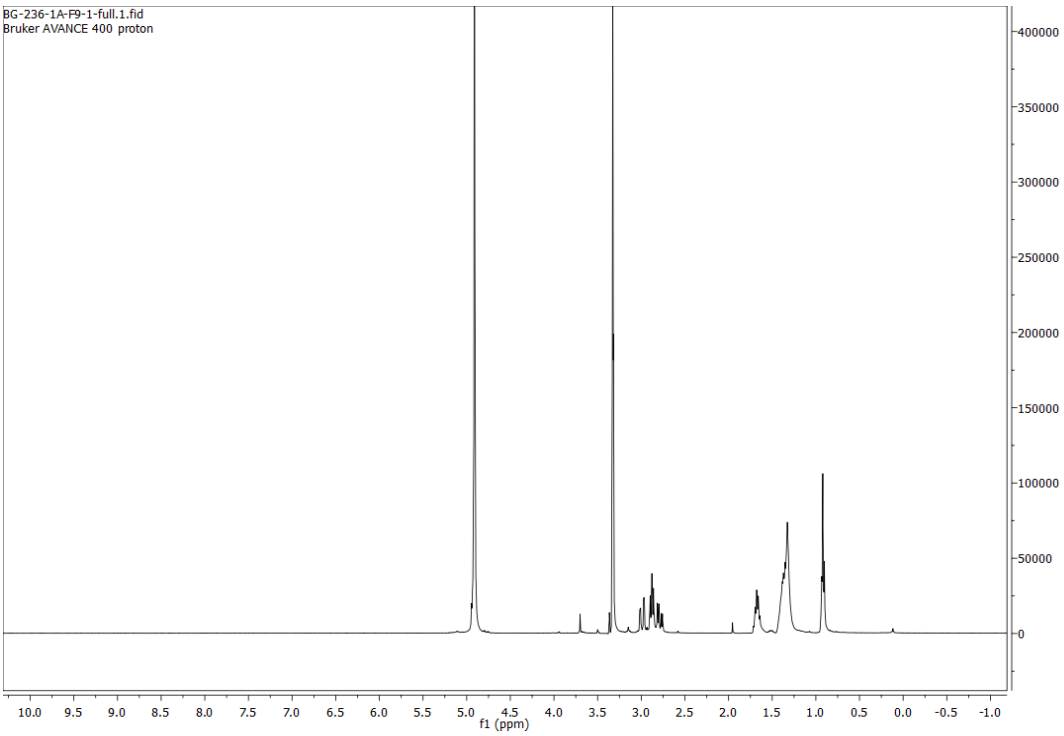

Figure S4. ^{13}C (100 MHz, CD_3OD) NMR spectrum for rhytismatone A (**1**)

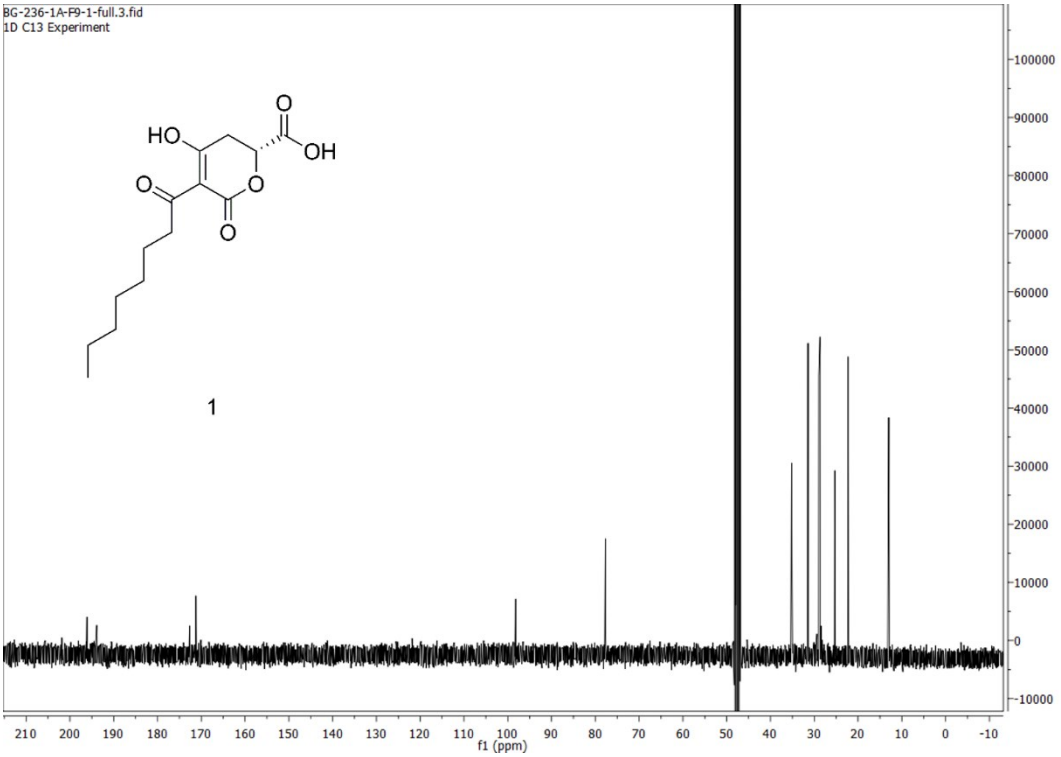

Figure S5. ^{1}H (400 MHz, CD_3OD) NMR spectrum for rhytismatone B (**2**)

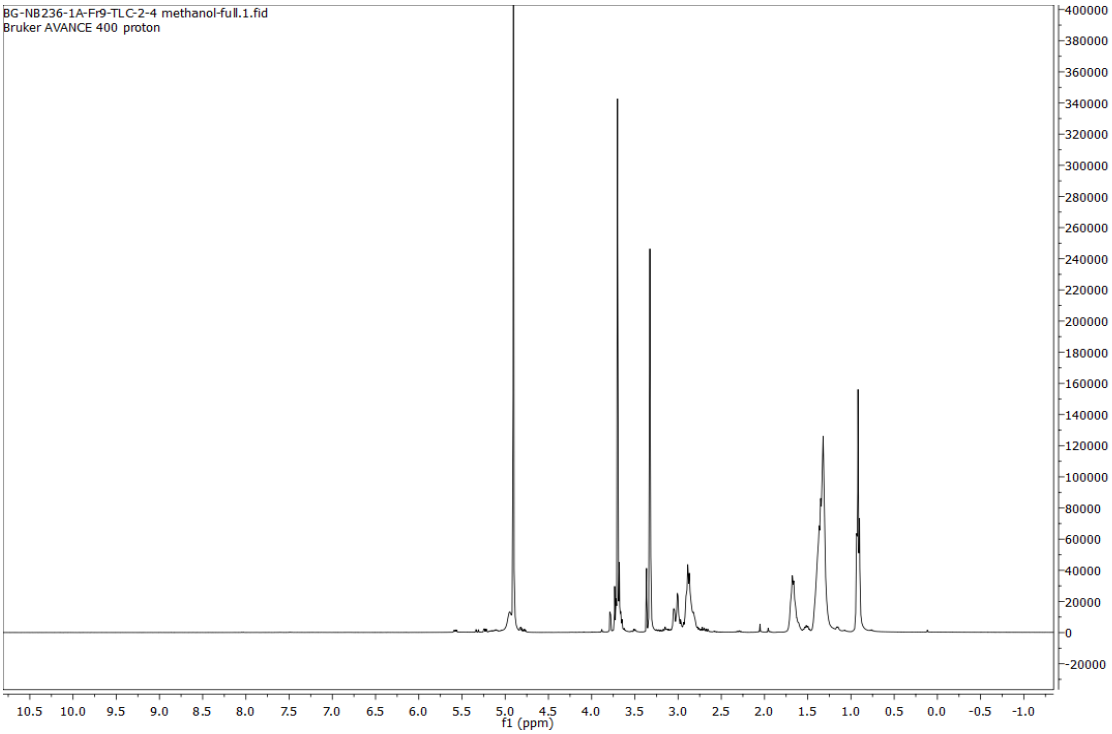

Figure S6. ^{13}C (100 MHz, CD_3OD) NMR spectrum for rhytismatone B (**2**)

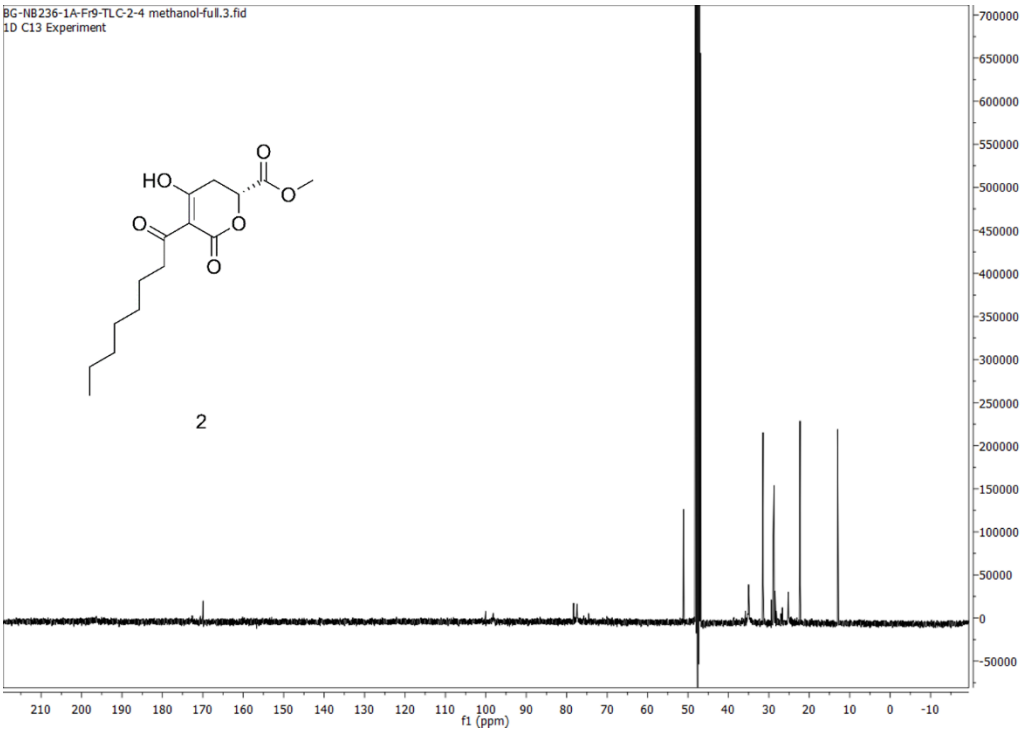

Figure S7. ^{1}H (400 MHz, CD_3OD) NMR spectrum for (**3**)

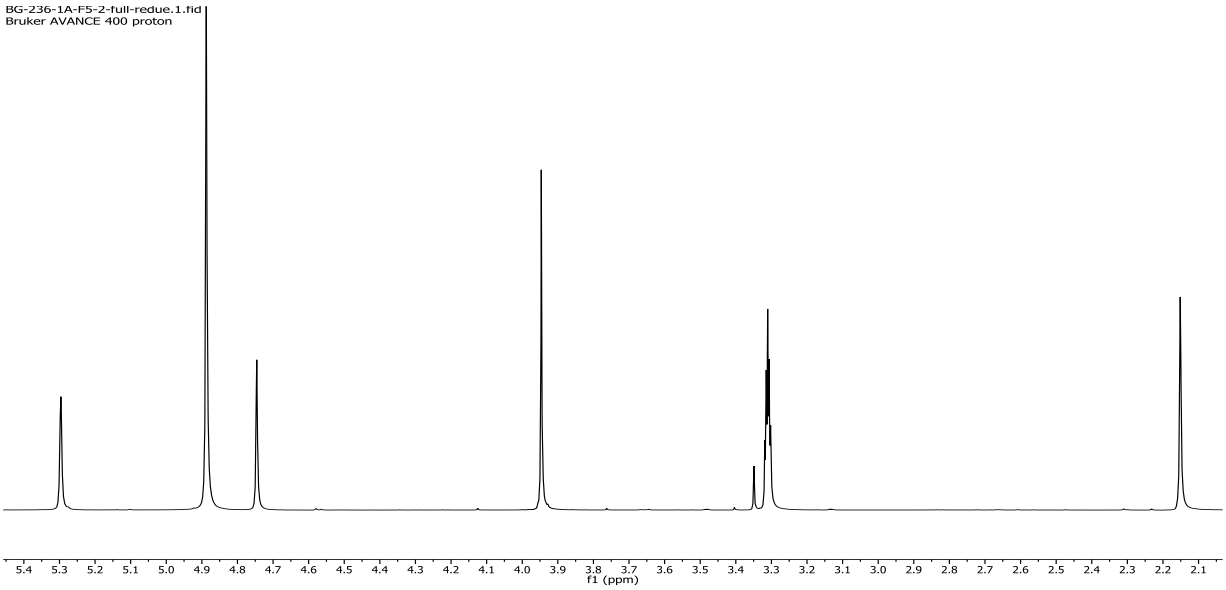

Figure S8. ^{13}C (100 MHz, CD_3OD) NMR spectrum for (**3**)

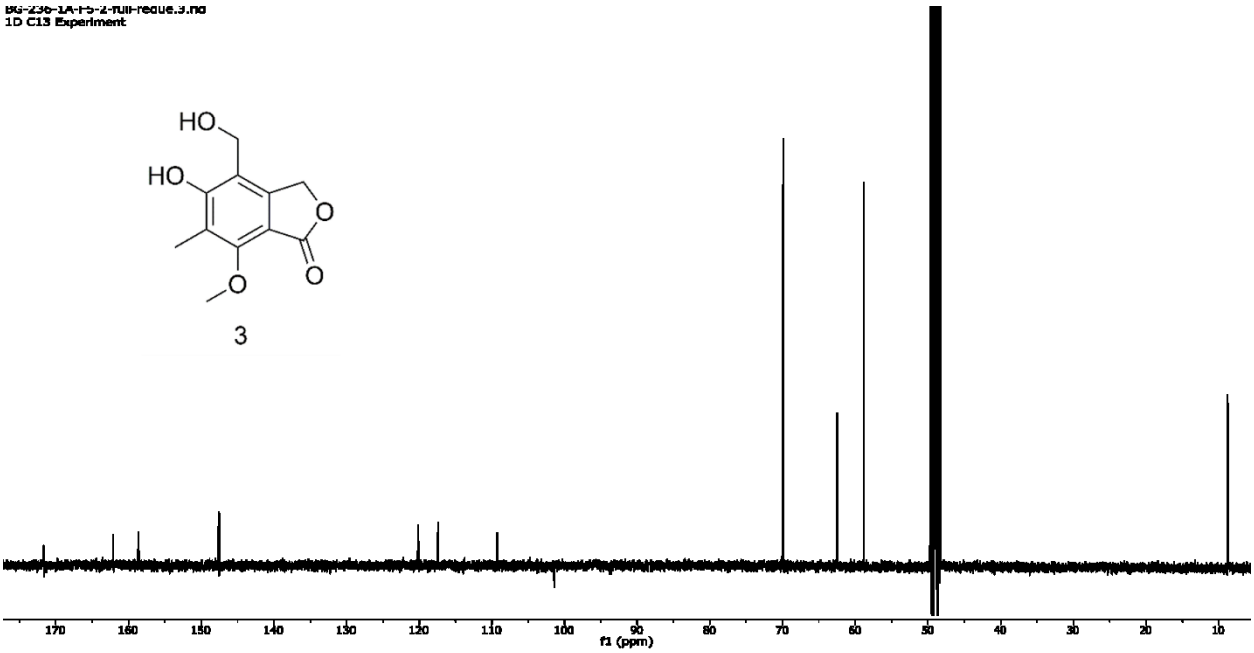

Figure S9. ^{1}H (400 MHz, CD_3OD) NMR spectrum for (**4**)

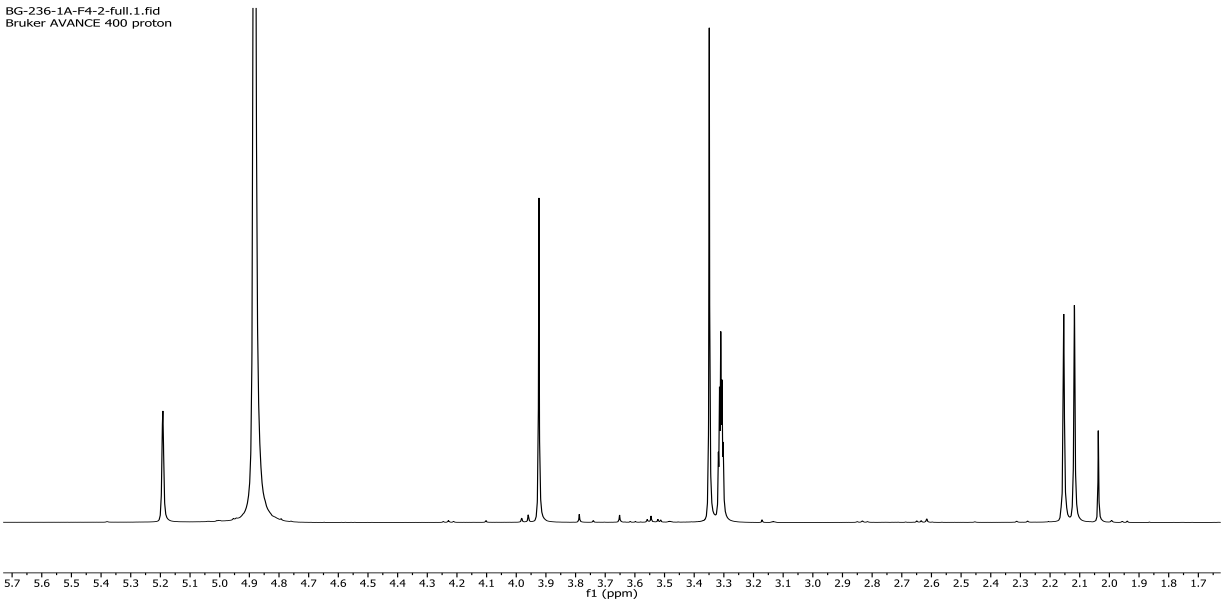

Figure S10. ^{13}C (100 MHz, CD_3OD) NMR spectrum for (**4**)

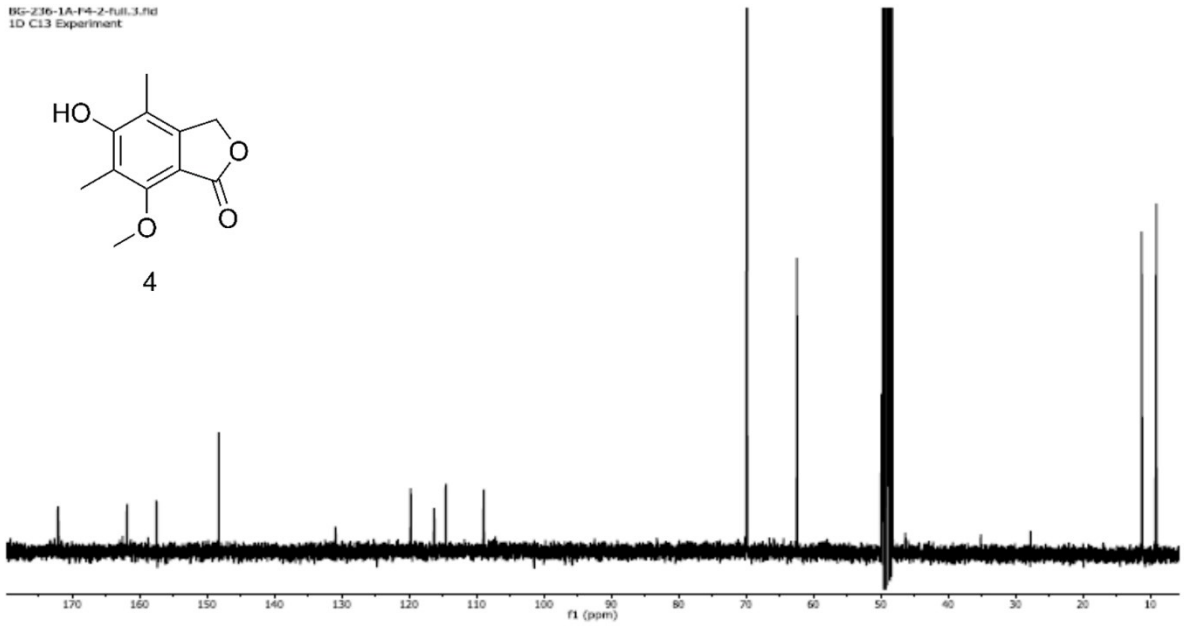

Figure S11. ^{1}H (400 MHz, CD_3OD) NMR spectrum for (**5**)

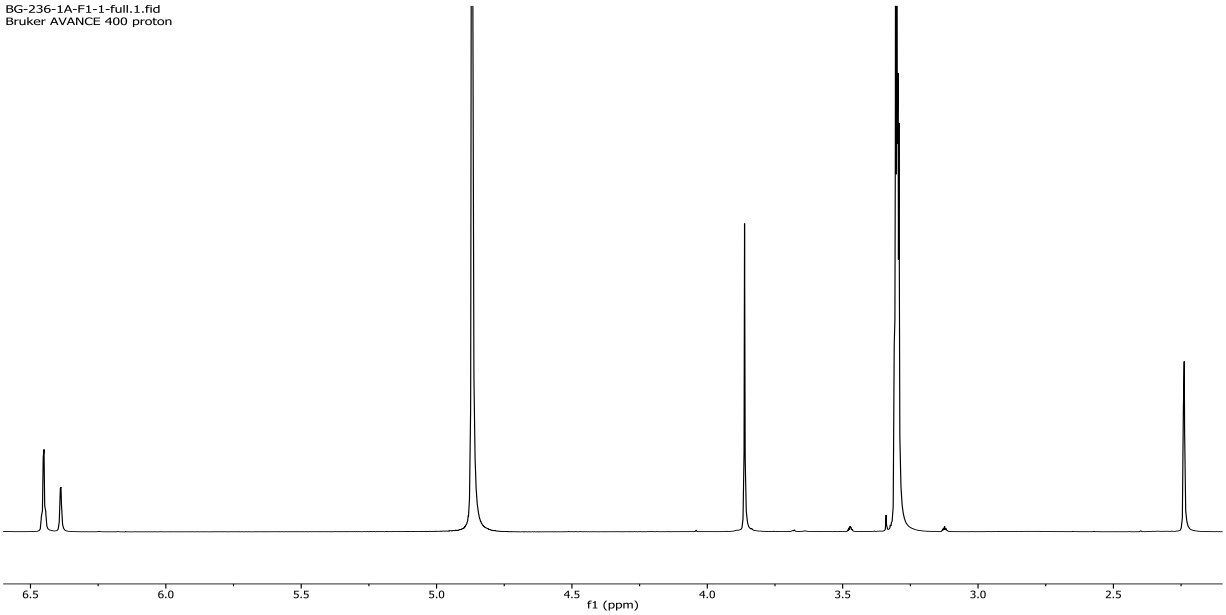

Figure S12. ^{13}C (100 MHz, CD_3OD) NMR spectrum for (**5**)

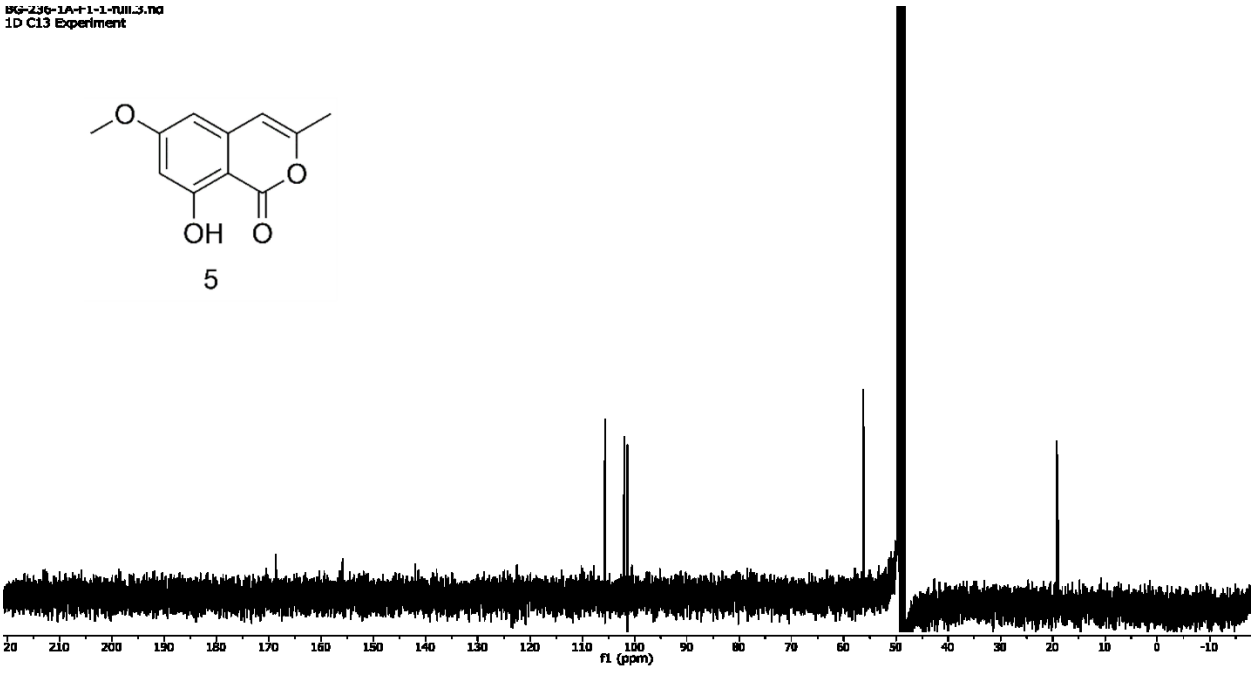

Figure S13. ^{1}H (400 MHz, CD_3OD) NMR spectrum for (**6**)

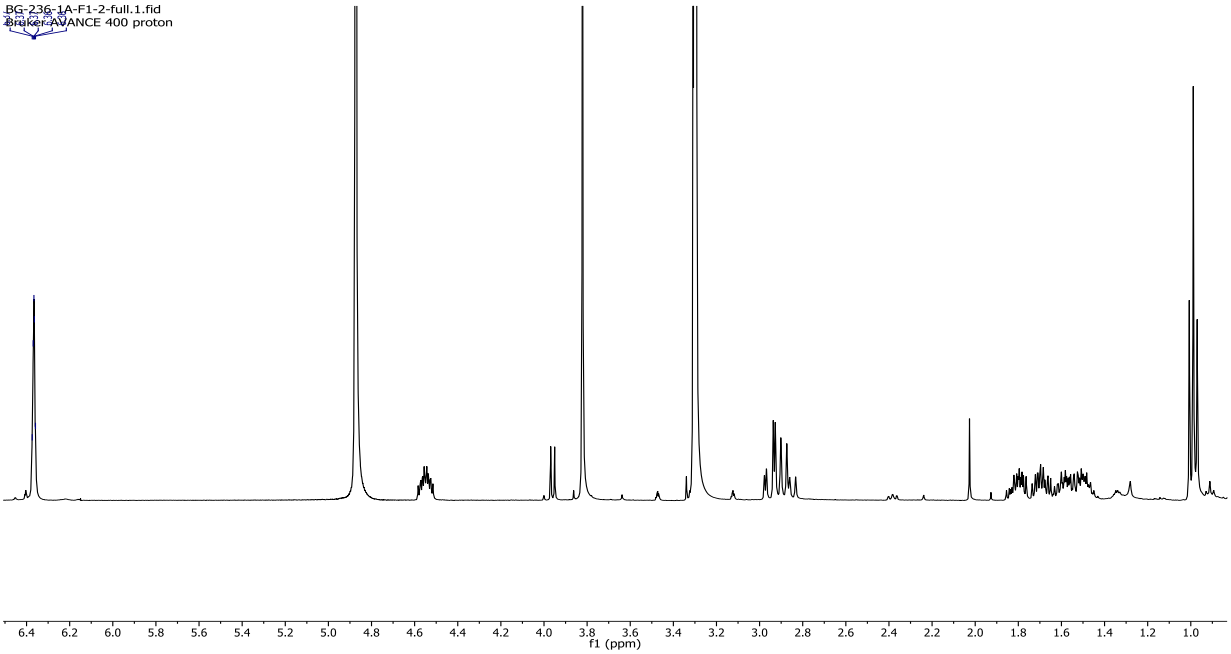

Figure S14. ^{13}C (100 MHz, CD_3OD) NMR spectrum for (**6**)

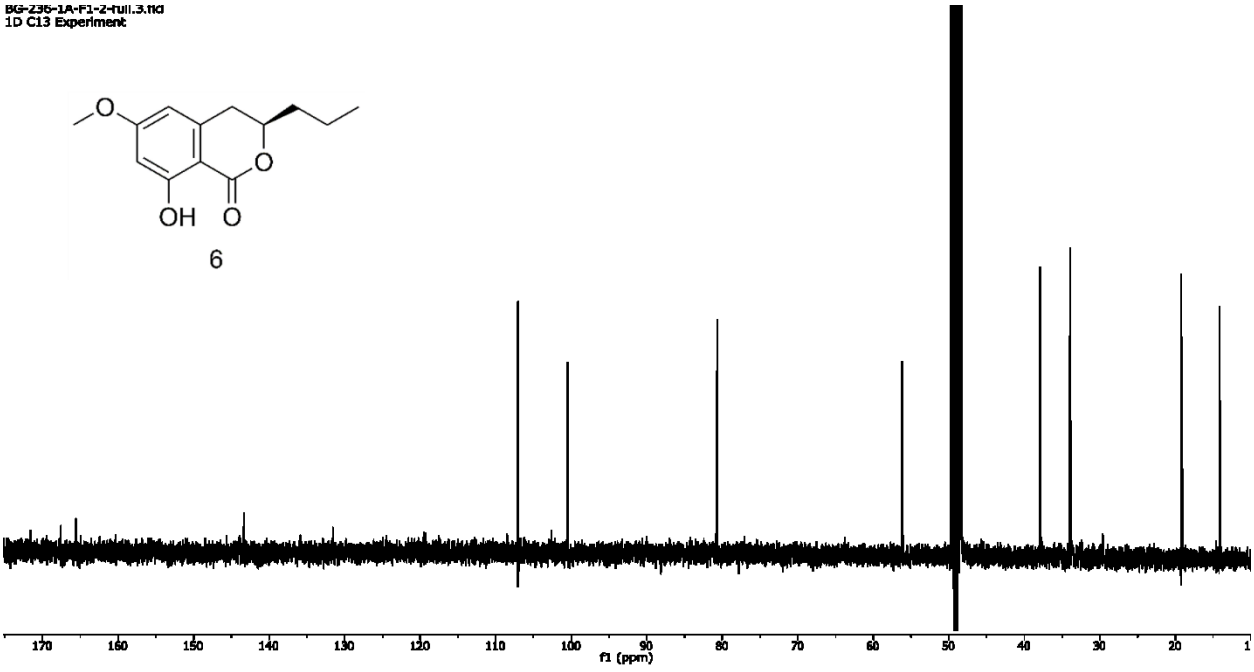

Figure S15. ^{1}H (400 MHz, CD_3OD) NMR spectrum for tyrosol (**7**)

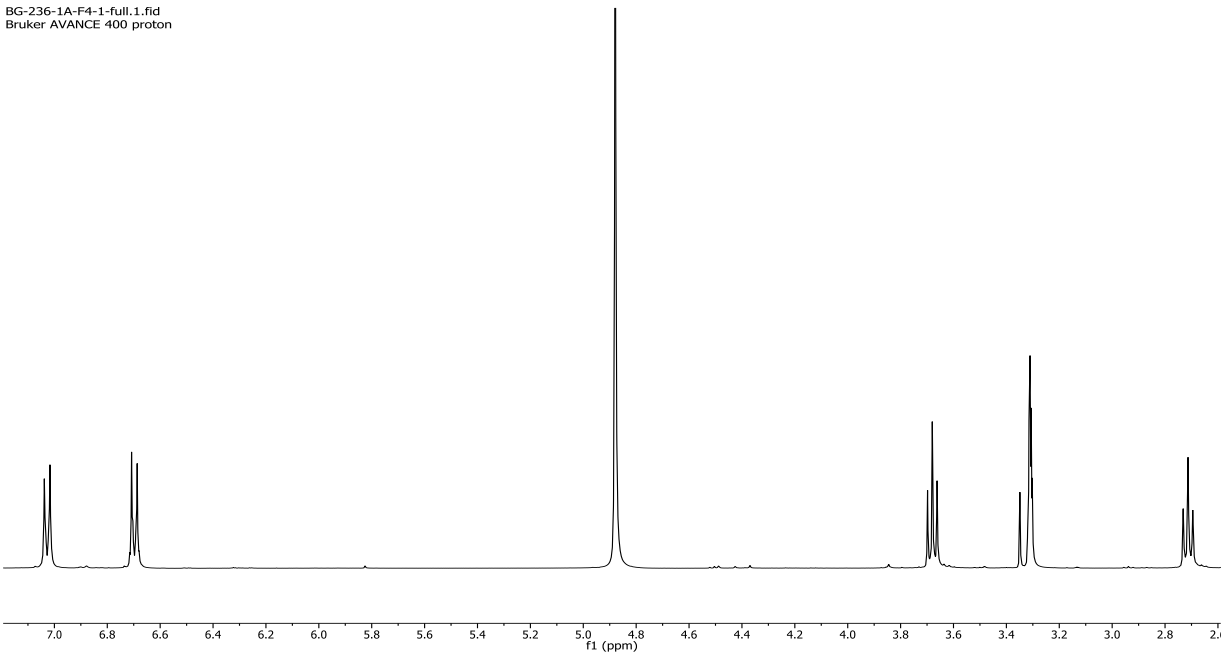

Figure S16. ^{13}C (100 MHz, CD_3OD) NMR spectrum for tyrosol (**7**)

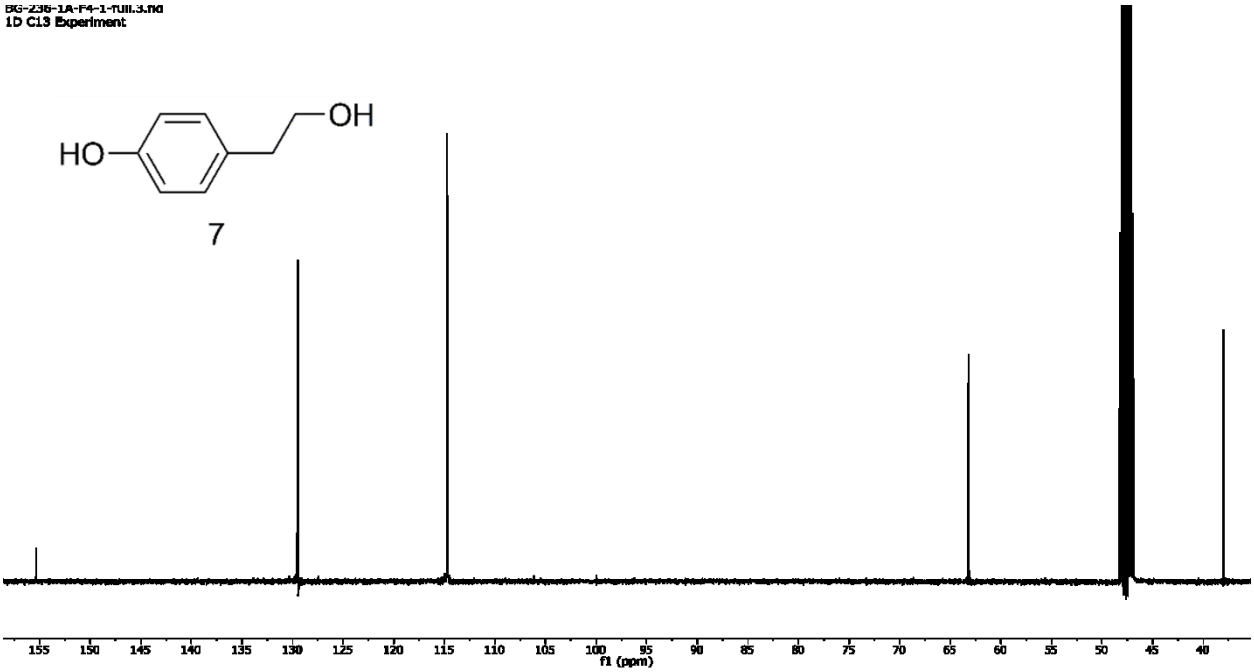

Figure S17. ^{1}H (400 MHz, CD_3OD) NMR spectrum for chloromycorrhizinone A (**8**)

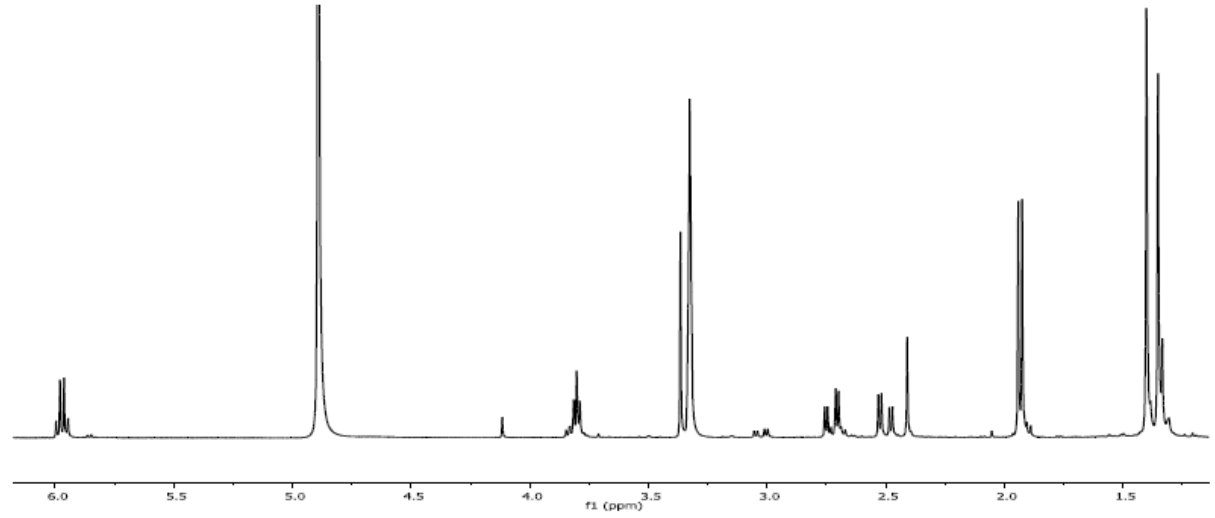

Figure S18. ^{13}C (100 MHz, CD_3OD) NMR spectrum for chloromycorrhizinone A (**8**)

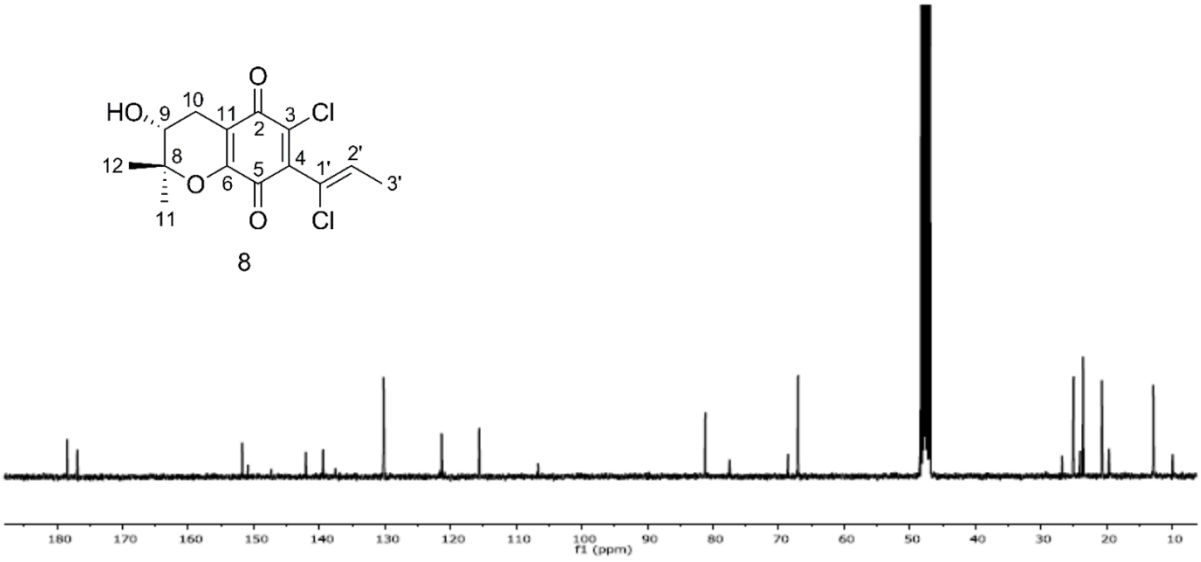

Figure S19. ^{1}H (400 MHz, CD_3OD) NMR spectrum for (1'*Z*)-dechloromycorrhizin A (**9**)

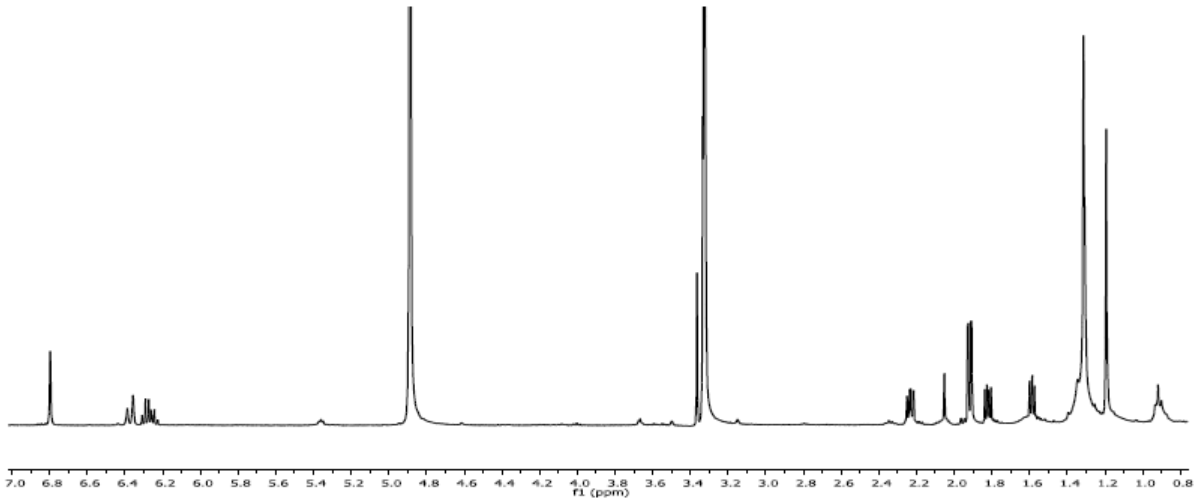

Figure S20. ^{13}C (100 MHz, CD_3OD) NMR spectrum for (1'*Z*)-dechloromycorrhizin A (**9**)

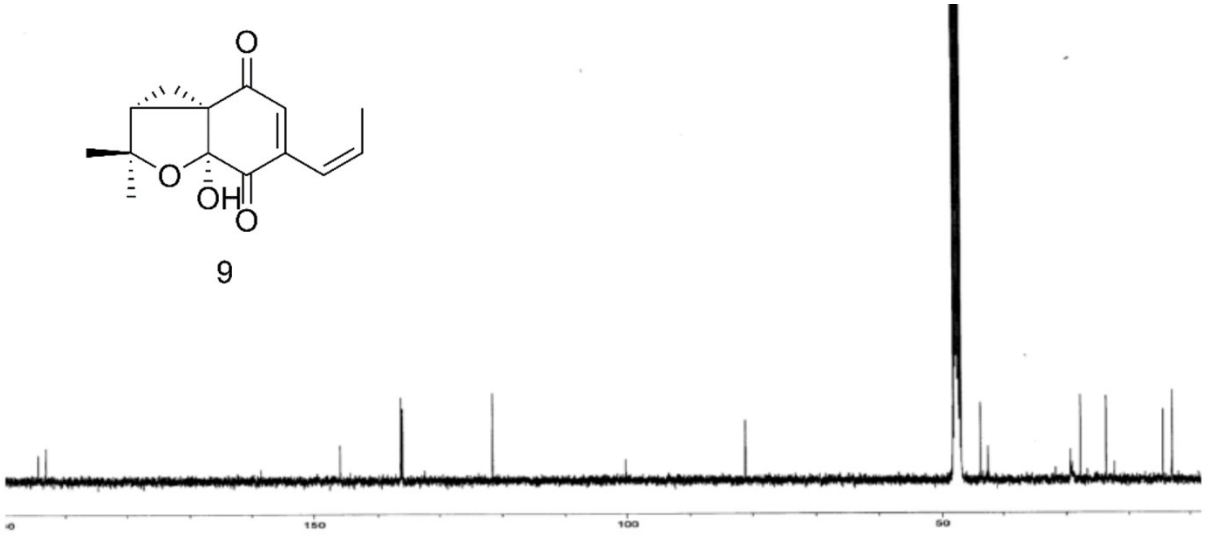

Figure S21. ^{1}H (400 MHz, CD_3OD) NMR spectrum for mycorrhizin A (**10**)

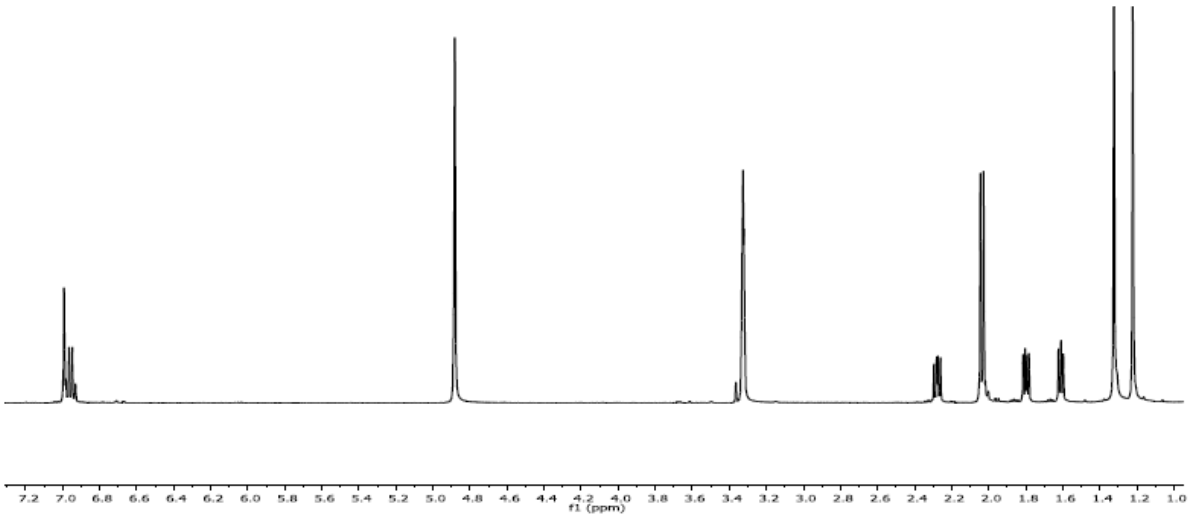

Figure S22. ^{13}C (100 MHz, CD_3OD) NMR spectrum for mycorrhizin A (**10**)

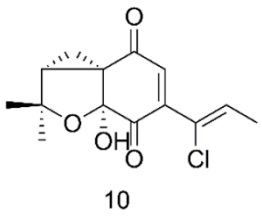

10

Figure S23. ^{1}H (400 MHz, CD_3OD) NMR spectrum for chloromycorrhizin A (**11**)

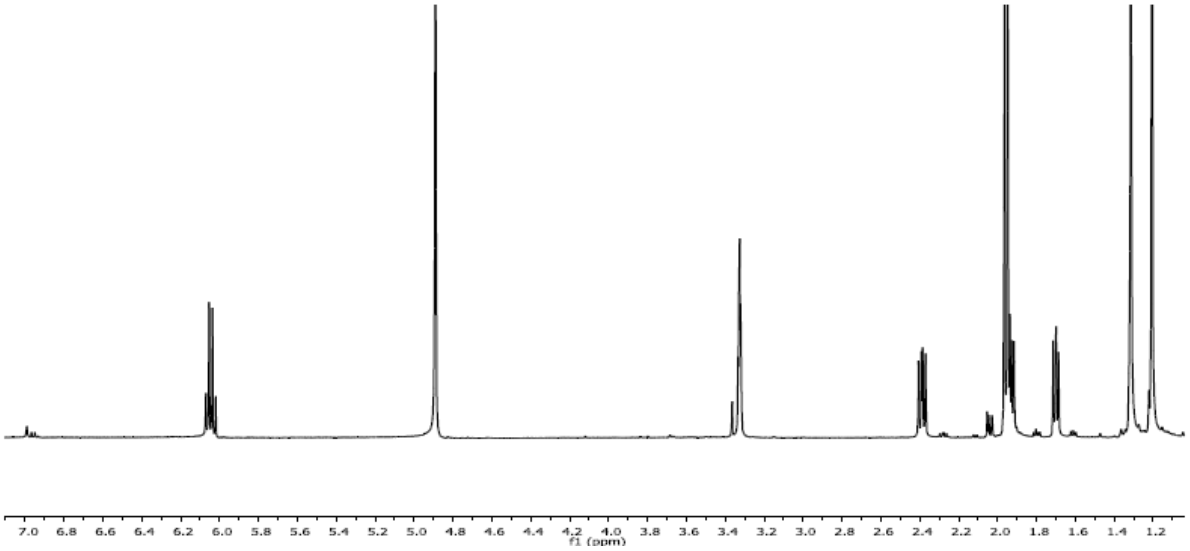

Figure S24. ^{13}C (100 MHz, CD_3OD) NMR spectrum for chloromycorrhizin A (**11**)

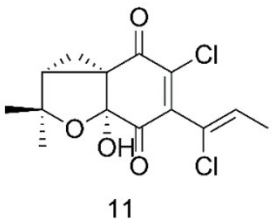

11

Figure S25. ^{1}H (400 MHz, CD_3OD) NMR spectrum for (**12**)

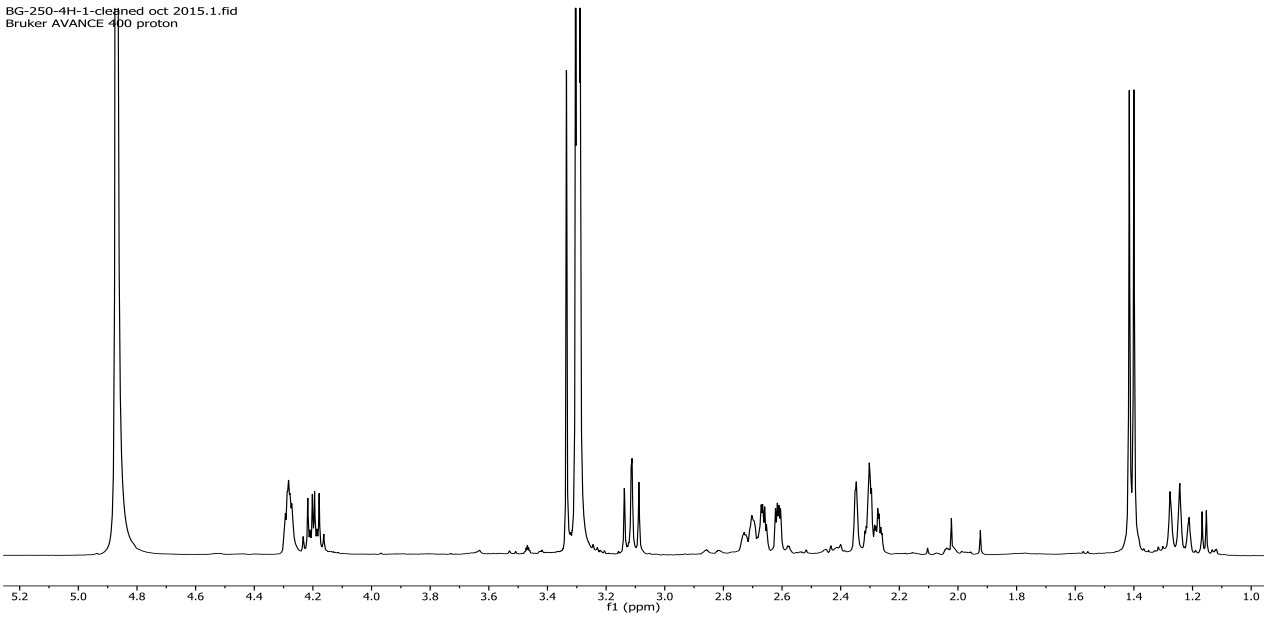

Figure S26. ^{13}C (100 MHz, CD_3OD) NMR spectrum for (**12**)

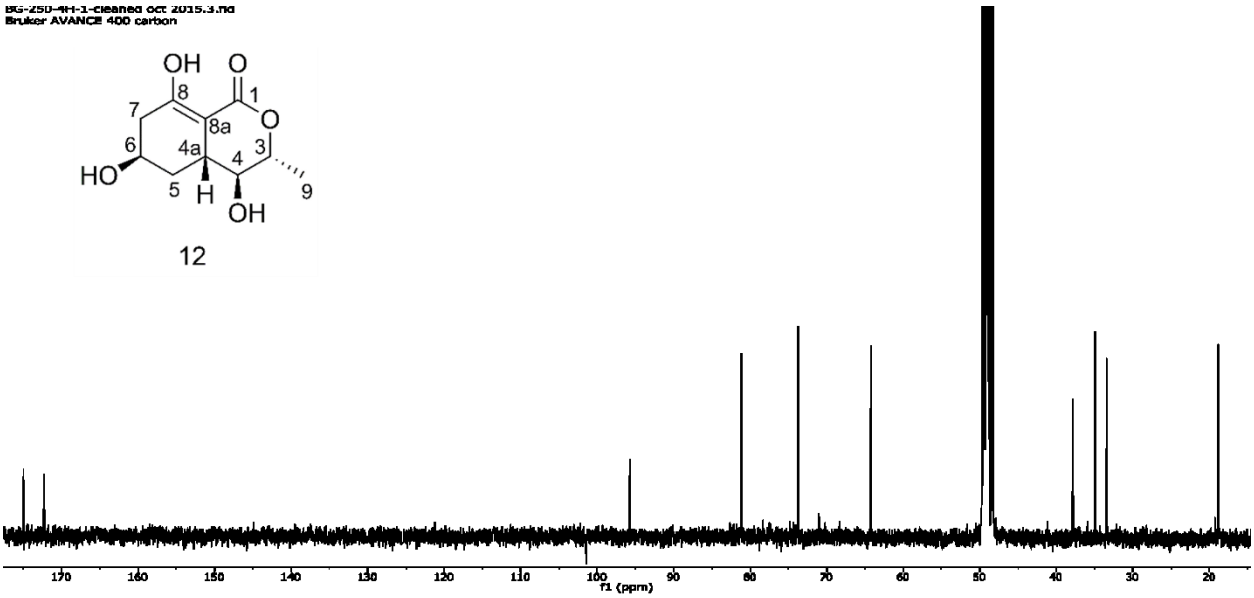

Figure S27. ^{1}H (400 MHz, CD_3OD) NMR spectrum for (**13**)

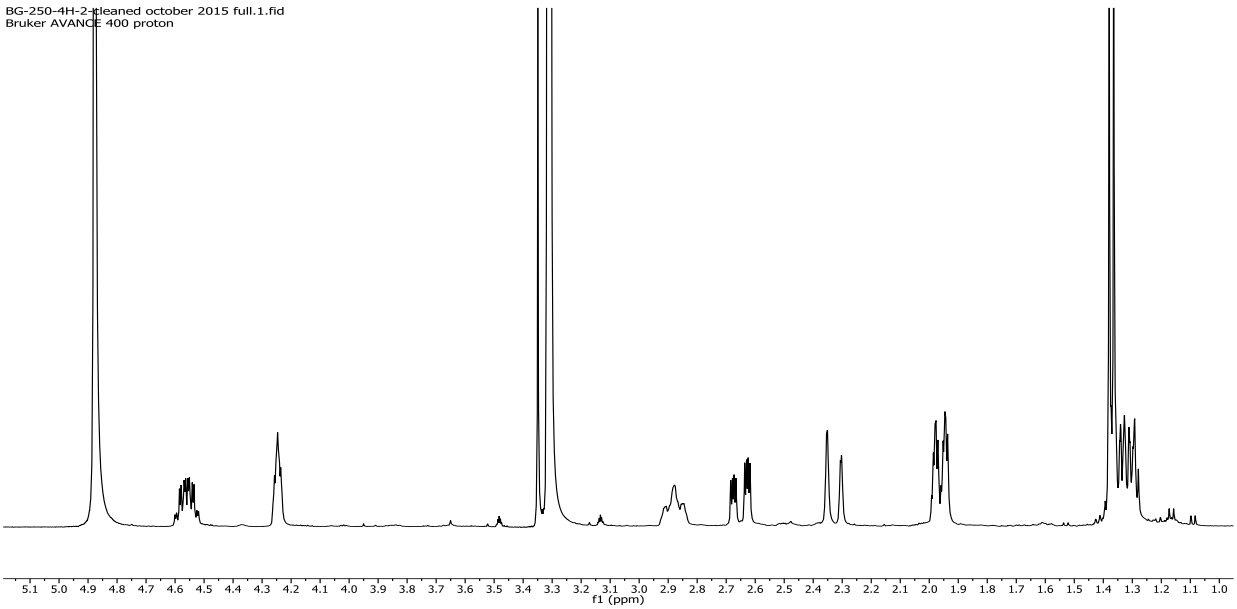

Figure S28. ^{13}C (100 MHz, CD_3OD) NMR spectrum for (**13**)

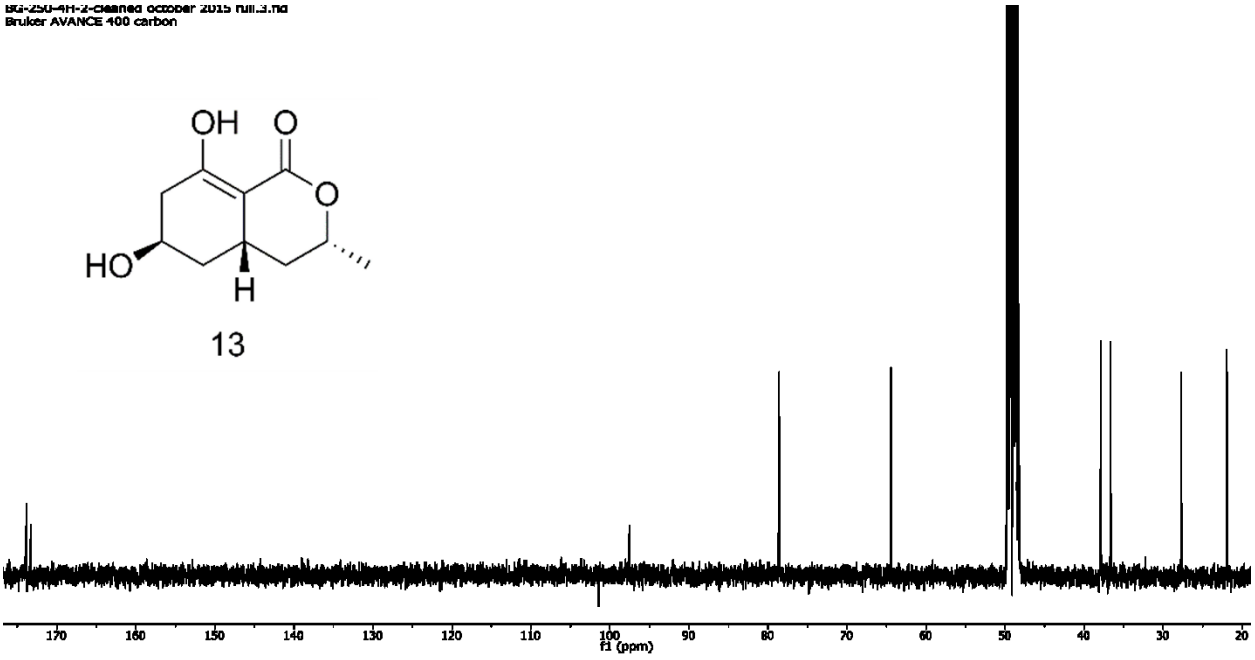

Figure S29. ^{1}H (400 MHz, CD_3OD) NMR spectrum for (**14**)

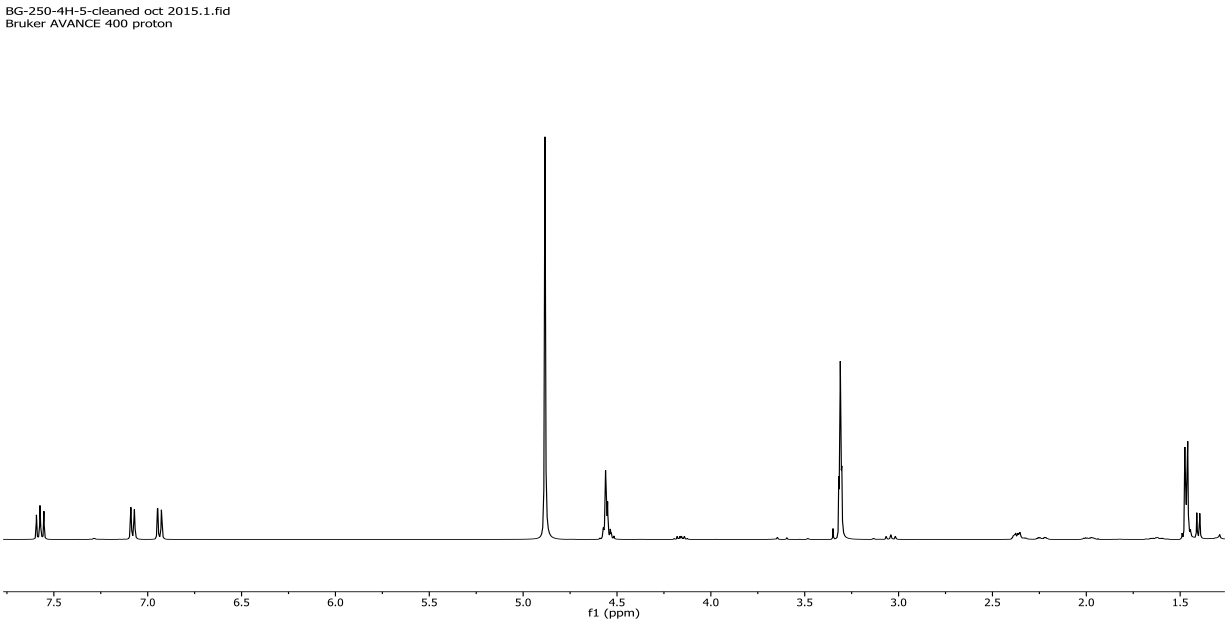

Figure S30. ^{13}C (100 MHz, CD_3OD) NMR spectrum for (**14**)

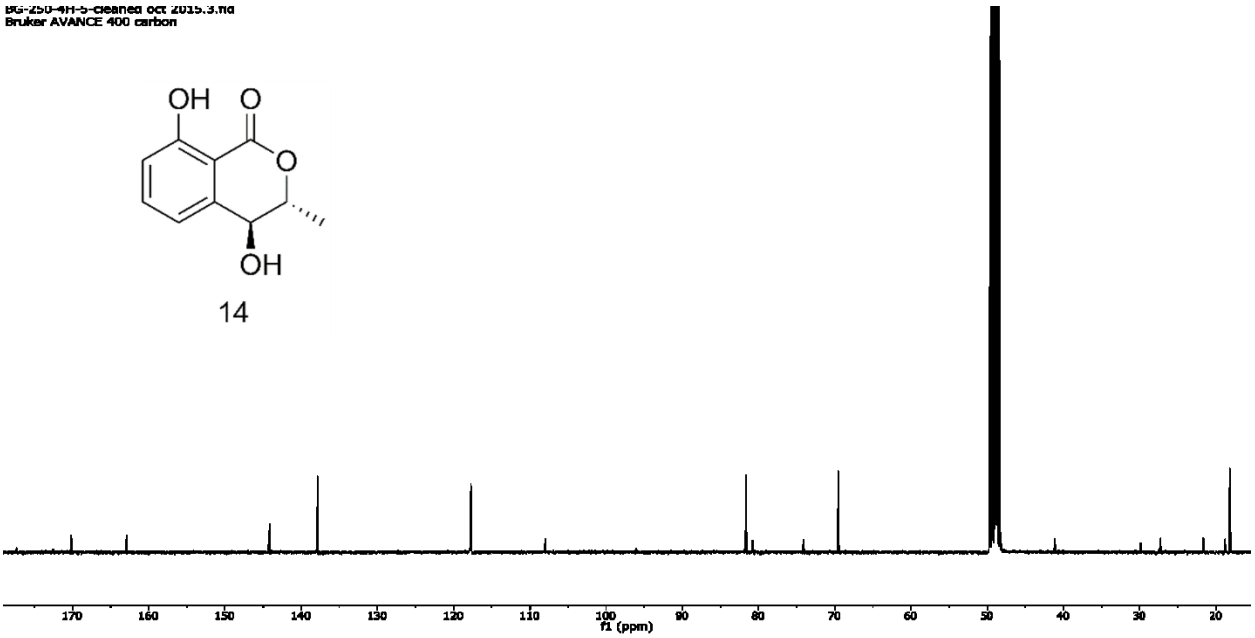

Figure S31. ^{1}H (400 MHz, CD_3OD) NMR spectrum for (**15**)

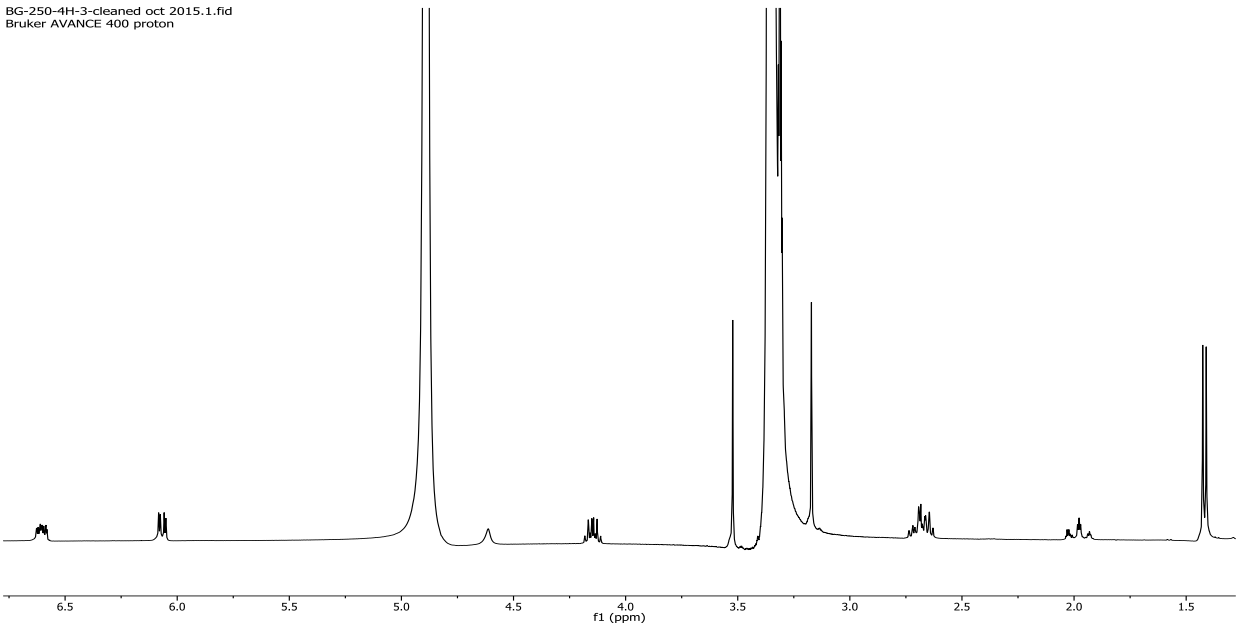

Figure S32. ^{13}C (100 MHz, CD_3OD) NMR spectrum for (**15**)

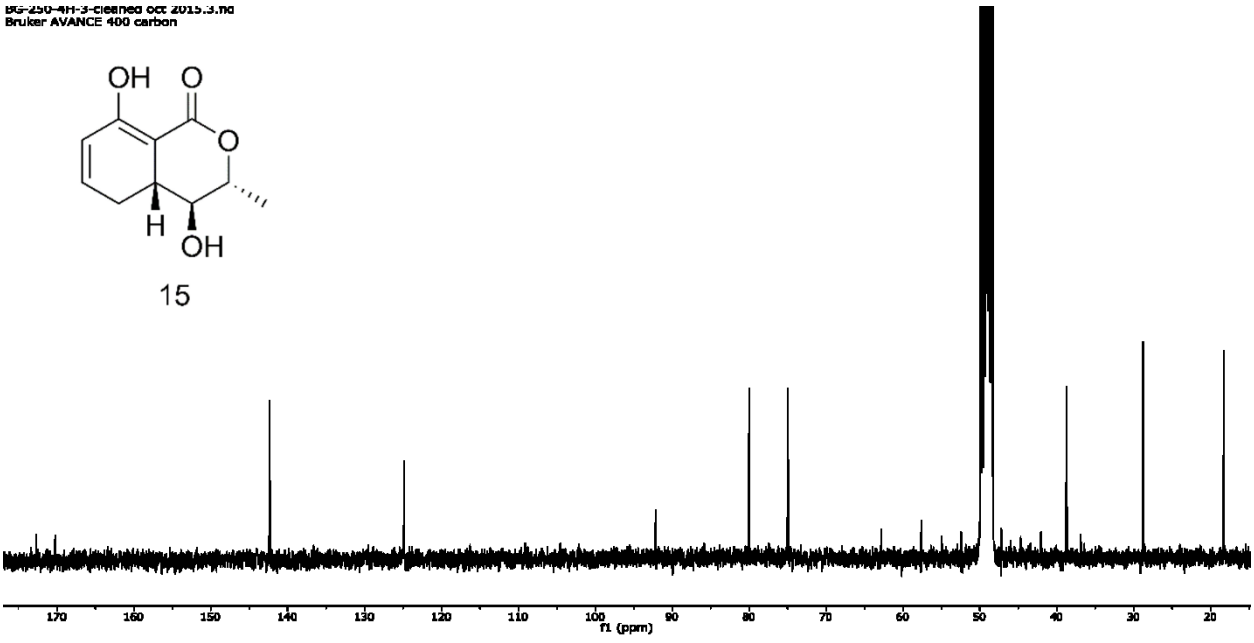

Figure S33. ^{1}H (400 MHz, CD_3OD) NMR spectrum for (**16**)

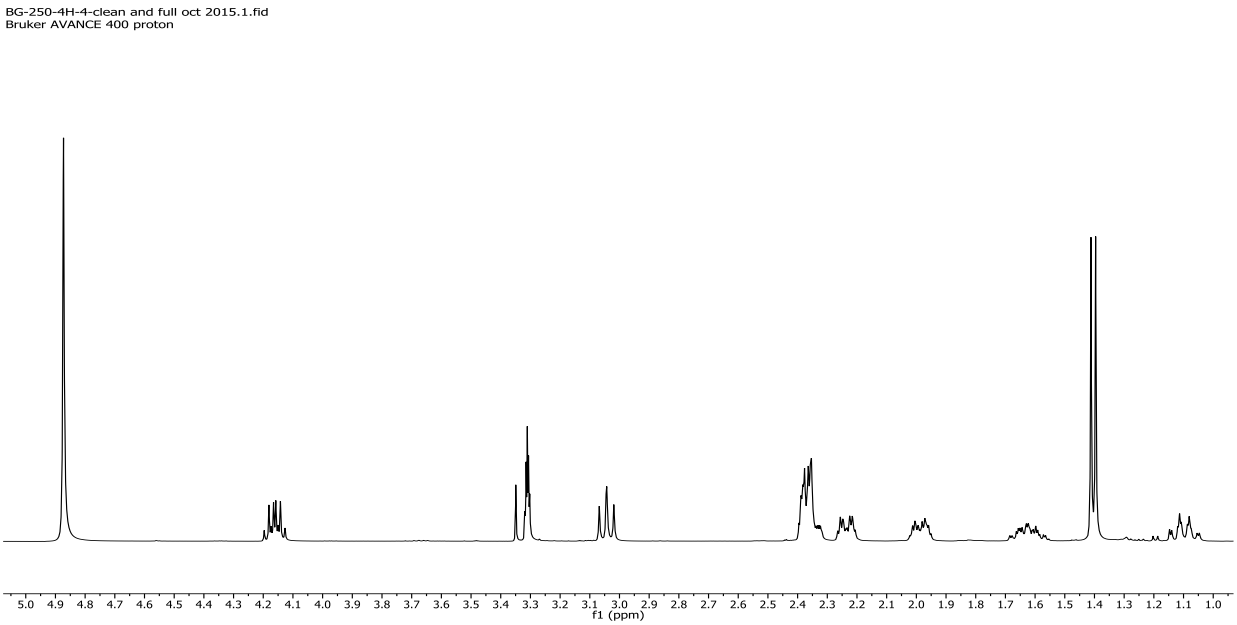

Figure S34. ^{13}C (100 MHz, CD_3OD) NMR spectrum for (**16**)

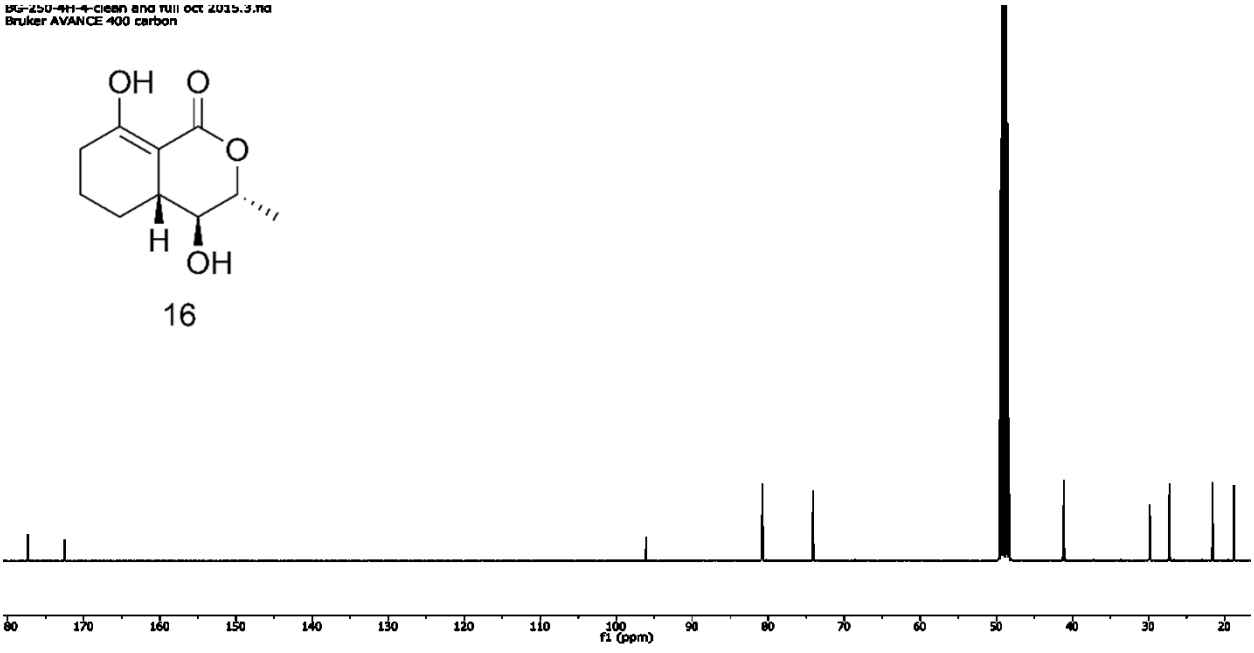

Figure S35. ^{1}H (400 MHz, CD_3OD) NMR spectrum for cryposporioposin (**17**)

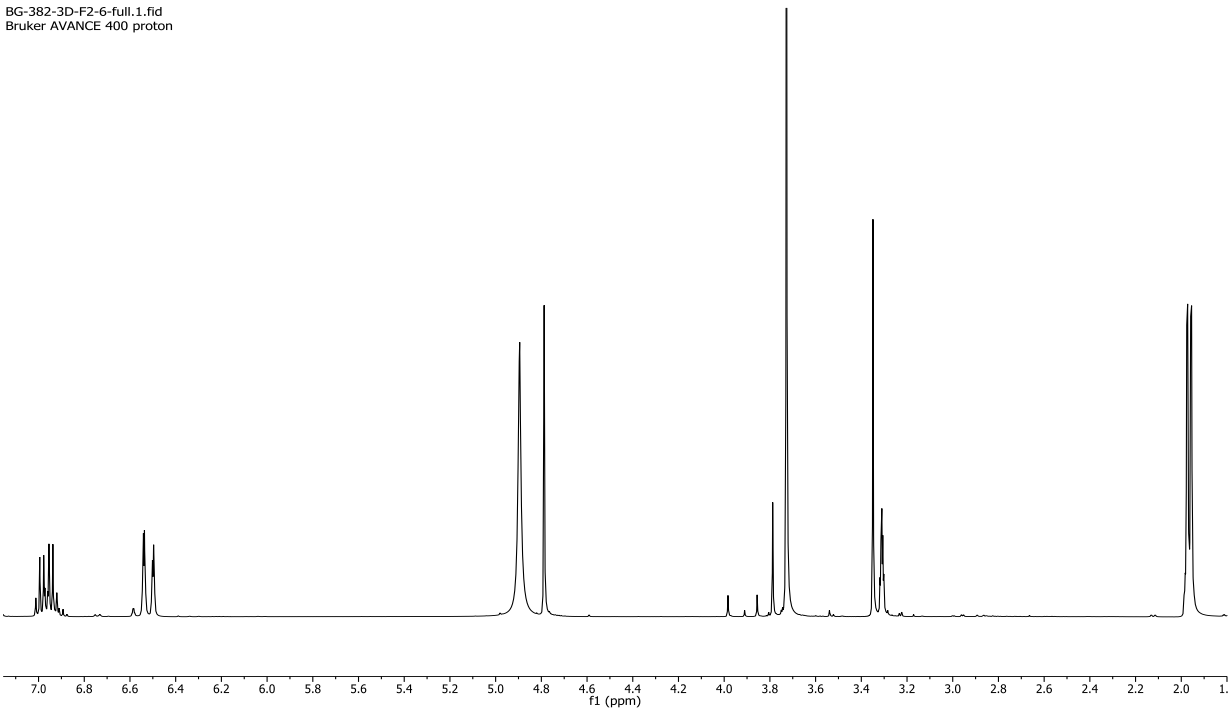

Figure S36. ^{13}C (100 MHz, CD_3OD) NMR spectrum for cryposporioposin (**17**)

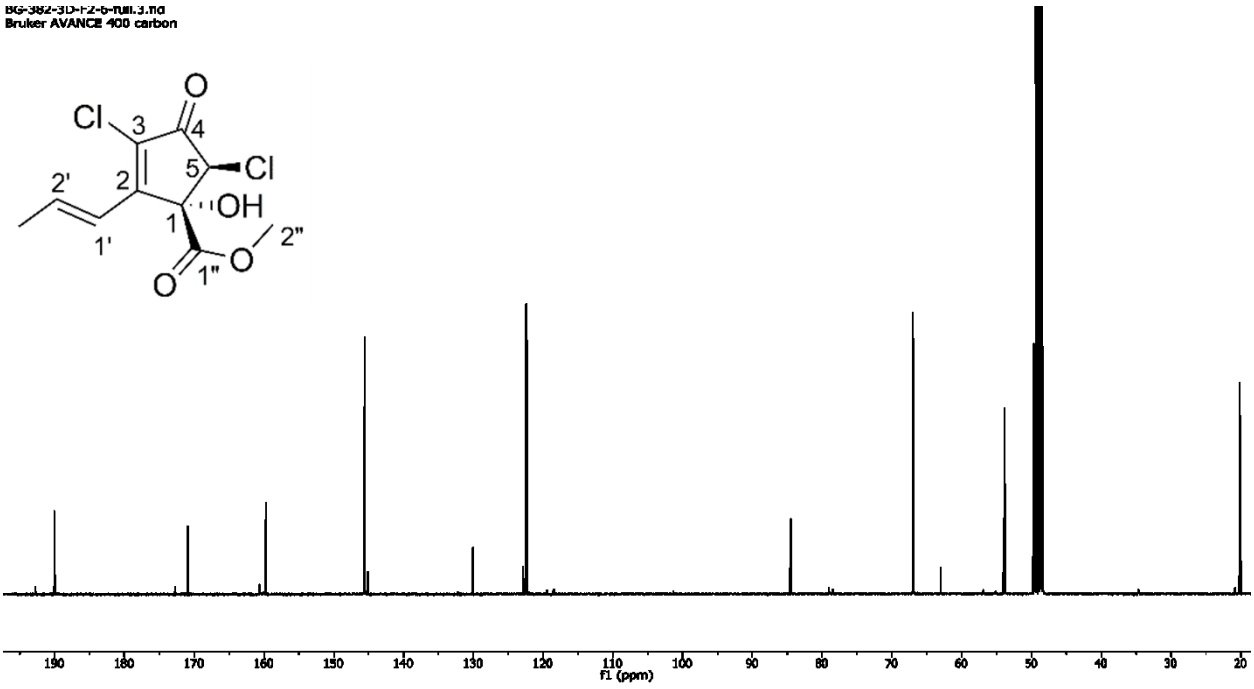

Figure S37. ^{1}H (400 MHz, CD_3OD) NMR spectrum for 5-hydroxy cryptosporiopsin (**18**)

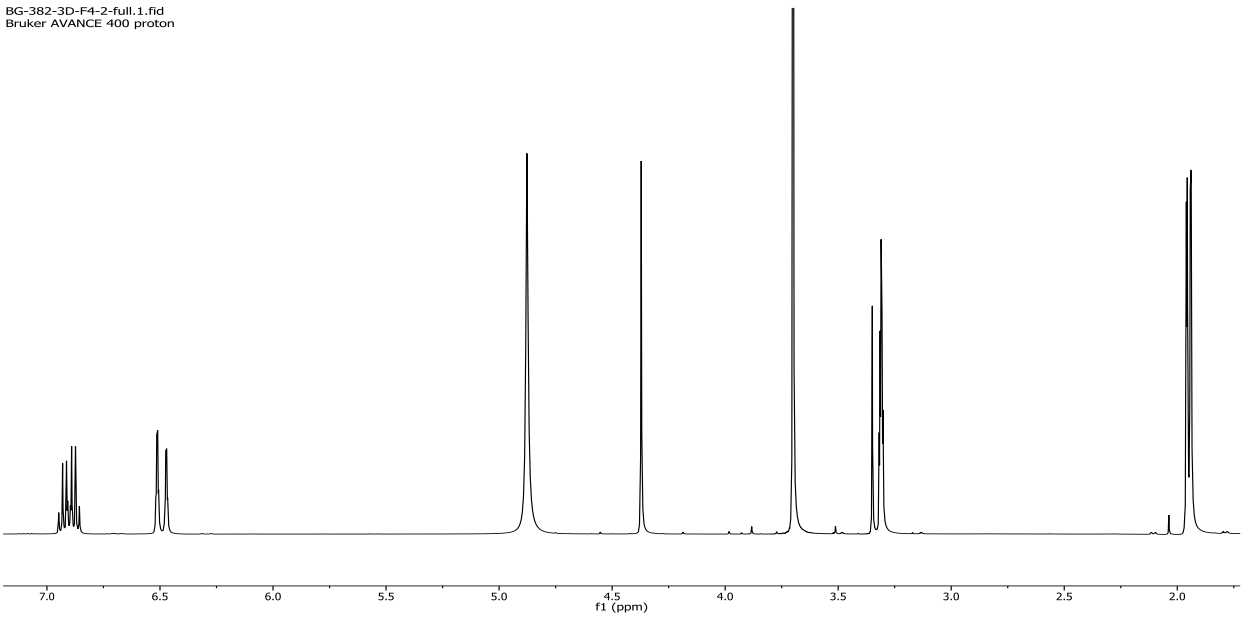

Figure S38. ^{13}C (100 MHz, CD_3OD) NMR spectrum for 5-hydroxy cryptosporiopsin (**18**)

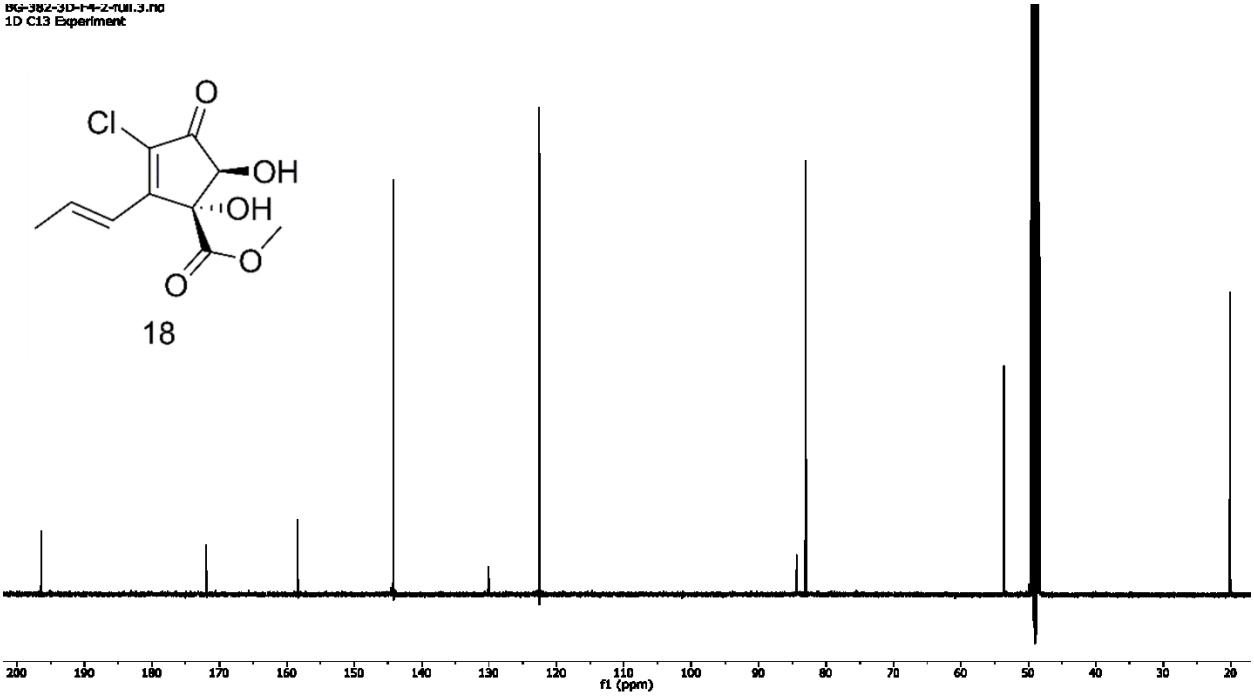

Figure S39. ^{1}H (400 MHz, CD_3OD) NMR spectrum for (+)-cryptosporiopsinol (**19**)

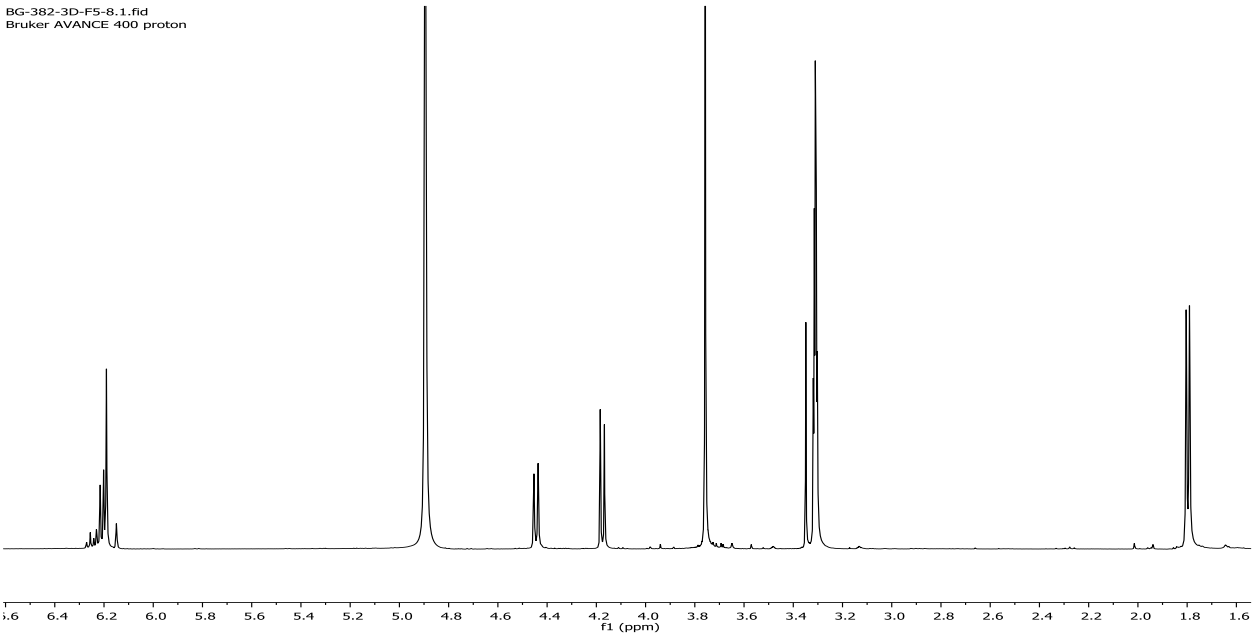

Figure S40. ^{13}C (100 MHz, CD_3OD) NMR spectrum for (+)-cryptosporiopsinol (**19**)

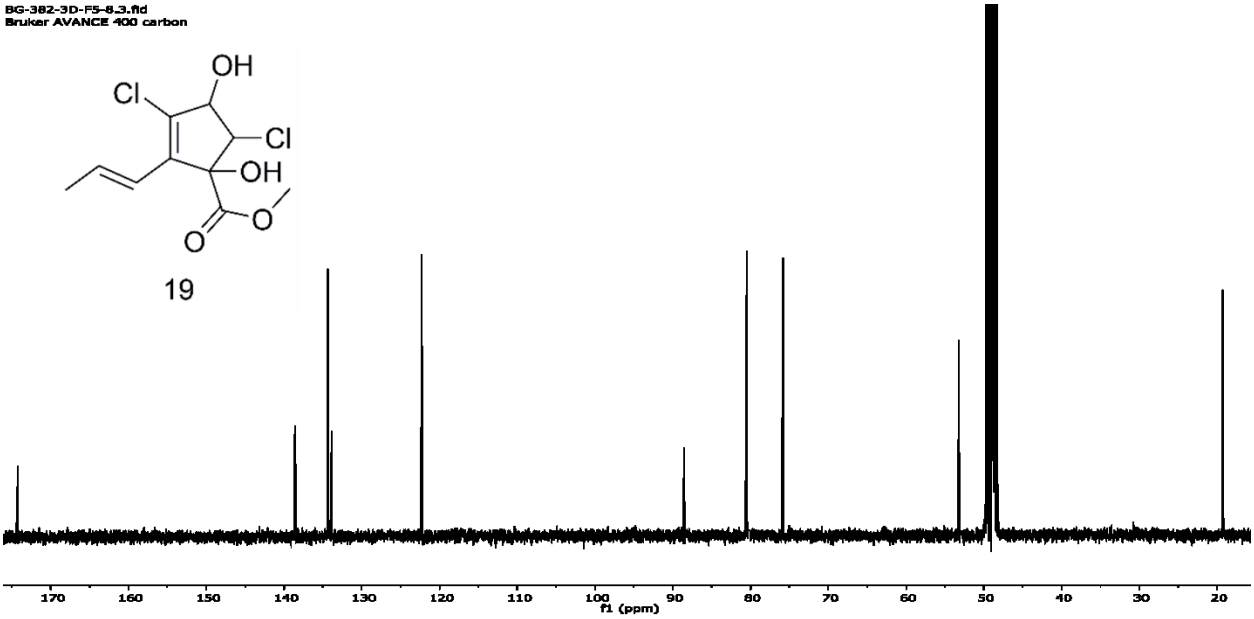

5-Hydroxy-7-methoxy-4,6-dimethylphthalide (**3**); 4.0 mg; white solid; UV (MeOH) λ_{max} (log ε) 230 (3.44), 265 (3.48); ^{1}H and ^{13}C NMR spectroscopic data are in accordance with the literature [59]; HRMS *m/z* 209.0808 $[M+H]^+$ (calc. for $[C_{11}H_{13}O_4]^+$ 209.0808).

5-Hydroxy-4-(hydroxymethyl)-7-methoxy-6-methylphthalide (**4**); 4.7 mg; white solid; UV (MeOH) λ_{max} (log ε) 230 (3.41), 265 (3.45); ^{1}H NMR spectroscopic data are in accordance with the literature[24]; HRMS *m/z* 225.0757 $[M+H]^+$ (calc. for $[C_{11}H_{13}O_5]^+$ 225.0758).

8-hydroxy-6-methoxy-3-methyisocoumarin (**5**); 2.3 mg; white solid UV (MeOH) λ_{max} (log ε) 240 (3.71), 277 (3.14), 327 (3.06); ^{1}H NMR spectroscopic data are in accordance with the literature[60]; HRMS *m/z* 207.0651 $[M+H]^+$ (calc. for $[C_{11}H_{11}O_4]^+$ 207.0652).

(R)-8-Hydroxy-6-methoxy-3-propylisochroman-1-one (**6**); 3.0 mg; light yellow solid; $[\alpha]^{25}_D$ – 8 (c 0.15, $CHCl_3$); UV (MeOH) λ_{max} (log ε) 222 (3.61), 267 (3.61), 302 (3.23); ^{1}H and ^{13}C NMR spectroscopic data are in accordance with the literature[4]; HRMS *m/z* 237.1119 $[M+H]^+$ (calc. for $[C_{13}H_{17}O_4]^+$ 237.1121).

Tyrosol (**7**); 5.4 mg; brown solid; UV (MeOH) λ_{max} (log ε) 230 (3.12), 278 (2.80); ^{1}H and ^{13}C NMR spectroscopic data are in accordance with the literature[4]; HRMS *m/z* 139.0754 $[M+H]^+$ (calc. for $[C_8H_{11}O_2]^+$ 139.0753).

(1'Z)-Dechloromycorrhizin A (**9**): 5.0 mg; yellow oil; $[\alpha]^{25}_D$ 39 (c 0.3, MeOH); UV (MeOH) λ_{max} (log ε) 220 (3.76); ^{1}H and ^{13}C NMR spectroscopic data are in accordance with the literature[33]; HRMS *m/z* 249.1125 $[M+H]^+$ (calc. for $[C_{14}H_{17}O_4]^+$ 249.1121).

Mycorrhizin A (**10**): 9.6 mg; yellow oil; $[\alpha]^{25}_D$ 29 (c 0.4, MeOH); UV (MeOH) λ_{max} (log ε) 230 (3.97), 300 (3.88); ^{1}H and ^{13}C NMR spectroscopic data are in accordance with the literature[61]; HRMS *m/z* 283.0733 $[M+H]^+$ (calc. for $[C_{14}H_{16}O_4Cl]^+$ 283.0732), HRMS *m/z* 283.0734 $[M+H]^+$ (calc. for $[C_{14}H_{16}O_4Cl]^+$ 283.0732).

Chloromycorrhizin A (**11**): 25.9 mg; yellow oil; $[\alpha]^{25}_D$ -35 (c 1.2, MeOH); UV (MeOH) λ_{max} (log ε) 250 (3.94), 305 (3.35); ^{1}H and ^{13}C NMR spectroscopic data are in accordance with the literature[61]; HRMS *m/z* 317.0345 $[M+H]^+$ (calc. for $[C_{14}H_{15}O_4Cl_2]^+$ 317.0342), HRMS *m/z* 317.0346 $[M+H]^+$ (calc. for $[C_{14}H_{15}O_4Cl_2]^+$ 317.0341).

6-hydroxyramulosin (**13**): 2.9 mg; clear solid; $[\alpha]^{25}_D$ 31.3 (c 0.06, $CHCl_3$); UV (MeOH) λ_{max} (log ε) 200 (3.10), 265 (3.60); for ^{1}H and ^{13}C NMR spectroscopic data, see Table 3; HRMS *m/z* 199.0963 $[M+H]^+$ (calc. for $[C_{10}H_{15}O_4]^+$ 199.0965).

(3R,4S)-4-hydroxymellein (**14**): 6.3 mg; white solid; $[\alpha]^{25}_D$ -13.8 (c 0.13, $CHCl_3$); UV (MeOH) λ_{max} (log ε) 220 (3.32), 245 (3.23), 315 (3.06); for ^{1}H and ^{13}C NMR spectroscopic data, see Table 3; HRMS *m/z* 195.0653 $[M+H]^+$ (calc. for $[C_{10}H_{11}O_4]^+$ 195.0652).

(3R,4S,4aR)-4,8-Dihydroxy-3-methyl-3,4,4a,5-tetrahydro-isochromen-1-one (**15**): 3.0 mg; clear solid; $[\alpha]^{25}_D$ 94.4 (c 0.03, $CHCl_3$); UV (MeOH) λ_{max} (log ε) 205 (3.41), 320 (3.36); ^{1}H

and ^{13}C NMR spectroscopic data are in accordance with the literature[39]; HRMS *m/z* 197.0809 $[M+H]^+$ (calc. for $[C_{10}H_{13}O_4]^+$ 197.0808).

(3R,4S,4aR)-4,8-Dihydroxy-3-methyl-3,4,4a,5,6,7-hexahydro-isochromen-1-one (**16**): 14.5 mg; white solid; $[\alpha]^{25}_D$ 10.9 (c 0.5, $CHCl_3$); UV (MeOH) λ_{max} (log ε) 200 (2.21), 265 (3.89); ^1H and ^{13}C NMR spectroscopic data are in accordance with the literature[39]; HRMS *m/z* 199.0963 $[M+H]^+$ (calc. for $[C_{10}H_{15}O_4]^+$ 199.0965).

Cryposporioposin (**17**): 37.4 mg; yellow solid; $[\alpha]^{25}_D$ 114.6 (c 1.71, MeOH); UV (MeOH) λ_{max} (log ε) 290 (4.06); for ^1H and ^{13}C NMR spectroscopic data, see supporting information Table S2; HRMS *m/z* 265.0028 $[M+H]^+$ (calc. for $[C_{10}H_{11}O_4Cl_2]^+$ 265.0029).

(1R,5S)-Methyl 3-chloro-1,5-dihydroxy-4-oxo-2-((E)-prop-1-en-1-yl)cyclopent-2-enecarboxylate (**18**): 13.8 mg; yellow solid; $[\alpha]^{25}_D$ 103.7 (c 0.64, MeOH); UV (MeOH) λ_{max} (log ε) 287 (4.00); for ^1H and ^{13}C NMR spectroscopic data, see supporting information Table S2; HRMS *m/z* 247.0368 $[M+H]^+$ (calc. for $[C_{10}H_{12}O_5Cl]^+$ 247.0368).

(+)-cryptosporiopsinol (**19**): 6.3 mg; clear solid; $[\alpha]^{25}_D$ 23.6 (c 0.16, MeOH); UV (MeOH) λ_{max} (log ε) 246 (5.08); for ^1H and ^{13}C NMR spectroscopic data, see supporting information Table S2; HRMS *m/z* 267.0186 $[M+H]^+$ (calc. for $[C_{10}H_{13}O_4Cl_2]^+$ 267.0185).

(R)-Mellein (**20**): HRMS *m/z* 179.0702 $[M+H]^+$ (calc. for $[C_{10}H_{11}O_3]^+$ 179.0702); for spectroscopic data, please refer to the literature.[4]

Table S2. ^1H (400 MHz) and ^{13}C (100 MHz) NMR data in CD_3OD for (+)-cryptosporiopsin (17), 5-hydroxy-cryptosporiposin (18) and (+)-cryptosporiopsinol (19) isolated from *P. sporulosa* DAOMC 250862

	17		**18**		**19**	
Position	**δ_C, type**	**δ_H (*J* in Hz)**	**δ_C, type**	**δ_H (*J* in Hz)**	**δ_C, type**	**δ_H (*J* in Hz)**
1	84.5, C		84.4, C		88.6, C	
2	159.7, C		158.4, C		138.6, C	
3	130.1, C		130.0, C		133.9, C	
4	190.0, C		196.5, C		75.9, CH	4.44, d (6.7)
5	67.0, CH	4.79, s	83.1, CH	4.37, s	80.5, CH	4.17, d (6.7)
1'	122.4, CH	6.52, dq (16.0, 1.7)	122.6, CH	6.49, dq (16.0, 1.7)	122.3, CH	6.19, o
2'	145.5, CH	6.96, dq (16.0, 7.0)	144.2, CH	6.90, dq (16.0, 6.9)	134.3, CH	6.15, o
3'	20.2, CH_3	1.96, dd (7.0, 1.7)	20.0, CH_3	1.95, dd (6.9, 1.7)	19.3, CH_3	1.8, d (5.3)
1"	171.0, C		171.9, C		174.3, C	
2"	53.8, CH_3	3.73, s	53.6, CH_3	3.70, s	53.3, CH_3	3.76, s

Appendix 1. Foliar endophytes studied for natural products

An unknown fungal species with an uncertain position within the family Rhytismataceae (Rhytismatales) was isolated as an endophyte of healthy *P. mariana* needles. The Rhytismataceae contains 55 genera and ca. 730 species of endophytic, parasitic, and saprotrophic plant-associates, many of which are exclusively associated with conifers.[62,63] This strain could not be identified to the genus or species rank based on ITS and LSU sequences. This is not surprising given the magnitude of this family and the paucity of reference sequences currently available. The ITS phylogeny places DAOMC 251461 in a polytomy including representative species of *Coccomyces*, *Colpoma*, *Lophodermium*, and *Therrya* species. These species are primarily associated with dead branches or foliage of conifer trees. Based on an ITS BLAST search, a closely related strain was reported as a *P. mariana* endophyte from Quebec, Canada [AY971725; identities = 427/431 (99%), gaps = 0/431 (0%)][64] (supporting information Figure S1).

Lachnum cf. *pygmaeum* DAOMC 250335 was isolated from ascospores originating from a collection of apothecia occurring on a dead *P. rubens* twig. This strain is referable to *L.* cf. *pygmaeum* based on apothecia morphology and ITS similarity with other *L. pygmaeum* sequences, e.g: AJ430219; identities = 475/476 (99%), gaps = 0/476 (0%). ITS BLAST results show a 99% similarity with several endophyte sequences derived from various plant (especially Ericaceae) root associates (e.g.: AY268215, EF026055, KJ817276, GQ996146) and forest soil (e.g.: KF617921). Several other *Lachnum* spp. strains were also isolated as *Picea* endophytes but did not produce active extracts in our assays (data not shown). DAOMC 250335 was collected as a saprotroph on a decomposing twig but was included in this study because of its close

relationship with plant root fungal associates and previous reports of biologically active metabolites from *Lachnum* spp.[32-34]

Based on ITS sequences, the *P. mariana* endophyte DAOMC 250863 is an undescribed Mycosphaerellaceae species, putatively a sister species *Phaeocryptopus gaeumannii* (*P. gaeumannii* GQ852752; identifies = 514/524 (98%), gaps = 0/524 (0%); supporting information Figure S2). *Phaeocryptopus gaeumannii* is a well-studied pathogen that causes Swiss needle cast of *Pseudotsuga menziesii*. This pathogen can reduce tree volume by up to 23–50%.[65-67] Despite its current designation in *Phaeocryptopus*, *P. gaeumannii* is phylogenetically unrelated to *Phaeocryptopus* s.s. (Dothideaceae) and is better placed within the Mycosphaerellaceae (Capdnodiales), therefore requiring taxonomic revision.[68] Mycosphaerellaceae sp. DAOMC 250863 was isolated as a *Picea rubens* needle endophyte during this ongoing survey and was also detected as a *P. mariana* endophyte in Quebec, where it comprised 11% of the total isolates on one study.[64]

Pezicula sporulosa DAOMC 250862 (Dermateaceae, Helotiales) was isolated as a *P. rubens* endophyte and shares a 100% similar ITS sequence with the *P. sporulosa* ex-type (NR_137161; CBS 224.96). *Pezicula* species occur as saprotrophs on recently dead branches and twigs and are reported, along with their *Cryptosporiopsis* asexual states, as endophytes or sometimes weak opportunistic pathogens capable of causing disease symptoms in weakened hosts.[69,70] *P. sporulosa* and related species are reported as branch, root, and foliar endophytes in conifers such as *Abies*, *Calocedrus*, *Chaemaecyparis*, *Juniperus*, *Picea, Pinus*, and *Thuja*.[71-75] Species isolated as foliar endophytes of conifers are not known to produce apothecia from foliage, but instead

produce them erumpent from recently dead twigs, branches, and stems of both conifer and hardwood trees, indicating their ability to infect various tissues from a wide range of hosts.[72,76]

References

(59) Katoh, N.; Nakahata, T.; Kuwahara, S. *Tetrahedron* **2008**, *64*, 9073–9077.
(60) Nozawa, K.; Nakajimi S.; Yamada, M.; Kawai, K-I. *Chem. Pharm. Bull.* **1980**, *28*, 1622–1625.
(61) Trofast, J.; Wickberg, B. *Tetrahedron* **1977**, *33*, 875–879.
(62) Kirk, P.; Cannon, P.; Minter, D.; Stalpers, J. *Dictionary of the Fungi 10th edn*. CABI, Wallingford, 2008.
(63) Lantz, H.; Johnston, P.; Park, D.; Minter, D.W. *Mycologia* **2011**, *103*, 57–74.
(64) Stefani, F.; Bérubé, *J. Botany* **2006**, *84*, 777–790.
(65) Maguire, D.A.; Kanaskie, A.; Voelker, W.; Johnson, R.; Johnson, G. West. *J. Appl. For*. **2002**, *17,* 86–95.
(66) Manter, D.K.; Bond, B.J.; Kavanagh, K.L.; Stone, J.K.; Filip, G.M. *Ecol. Model*. **2003**, *164,* 211–226.
(67) Ritóková, G,; Shaw, D.C.; Filip, G.; Kanaskie, A.; Browning, J.; Norlander, D. *Forests* **2016**, *7,* 155.
(68) Winton, L.M.; Stone, J.K.; Hansen, E.M.; Shoemaker, R. *Mycologia* **2007**, *99*, 240–252.
(69) Verkley, G.J.M. *Stud. Mycol.* **1999**, *44*, 1–180.
(70) Lynch, S.C.; Zambino, J.S.; Wang, D.H.; Eskalen, A. *Plant Dis.* **2013**, *97*, 1025–1036.
(71) Petrini, O.; Carroll, G. *Can. J. Bot*. **1981**, *59*, 629–636.
(72) Holdenrieder, O.; Sieber, T.N. *Mycol. Res*. **1992**, *96,* 151–156.
(73) Kowalski, T.; Zych, P. *Osterr. Z. Pilzkd*. **2002**, *11*, 107–116.
(74) Yuan, Z-L.; Rao, L-B.; Chen, Y-C.; Zhang, C-L.; Wu, Y-G. *Fungal Biol*. **2011**, *115,* 197–213.
(75) Yuan, Z.; Verkley, G.J. *Mycoscience* **2015**, *56,* 205–213.
(76) Chen, C.; Verkley, G.J.; Sun, G.; Groenewald, J.Z.; Crous, P.W. *Fungal Biol*. **2016**, *120*, 1291–1322.